Article

How Can Climate Resilience Be Measured and Visualized? Assessing a Vague Concept Using GIS-Based Fuzzy Logic

Mathias Schaefer [1,]* , **Nguyen Xuan Thinh [1] and Stefan Greiving [2]**

[1] Department of Spatial Information Management and Modelling (RIM), TU Dortmund University, 44227 Dortmund, Germany; nguyen.thinh@tu-dortmund.de
[2] Institute of Spatial Planning (IRPUD), TU Dortmund University, 44227 Dortmund, Germany; stefan.greiving@tu-dortmund.de
[*] Correspondence: mathias.schaefer@tu-dortmund.de

check for
updates

Abstract: As negative impacts of climate change tend to increase in the future, densely-populated cities especially need to take action on being robust against natural hazards. Consequently, there is a growing interest from scientists in measuring the climate resilience of cities and regions. However, current measurements are usually assessed on administrative levels, not covering potential hotspots of hazardous or sensitive areas. The main aim of this paper focusses on the measurement of climate resilience in the City of Dortmund, Germany, using Geographic Information Systems (GIS). Based on a literature review, we identified five essential components of climate resilience and initially designed a theoretical framework of 18 indicators. Since climate resilience is still a vague concept in scientific discourses, we implemented local expert knowledge and fuzzy logic modelling into our analysis. The benefit of this study not only lies in the fine-scale application, but also in the relevance for multiple disciplines by integrating social and ecological factors. We conclude that climate resilience varies within the city pattern, with the urban core tending to be less resilient than its surrounding districts. As almost the entire geodata set used is freely available, the presented indicators and methods are to a certain degree applicable to comparable cities.

Keywords: climate resilience; sustainable development; urban planning; remote sensing; fuzzy logic; compromise programming

1. Introduction

The worldwide issue of climate change, population growth and environmental pollution is becoming increasingly apparent to the general public—including the youth—and is discussed controversial via social media [1,2]. However, it is empirically documented that urban agglomerations with high population densities are particularly confronted with air and noise pollution, urban heat islands' effects due to a lack of green spaces, or flash floods enforced by ongoing surface sealing processes. Despite these circumstances, it is also expected that 68% of the world's population by the year 2050 will live in cities, which probably reinforces the above issues [3]. It is plausible that in the case of an extreme event many people and infrastructures in large cities are affected at once, as they are cumulated in a relatively small space, which also triggers cascading effects such as disruptions of supply chains which leads to negative economic impacts. With economic losses of over 96 billion euros due to climate-related extremes between 1980–2017, Germany is ranked on the first place in the Europe Economic Area (EEA) [4]. In addition, in 2003 and 2018, Germany had its two hottest and driest meteorological summers since the beginning of systematic weather records in 1881 [5,6].

Whenever current debates on climate change and extreme weather events are discussed in the context of urban planning, the concept of climate resilience is often echoed by politicians and scientists. In brief, a climate resilient city has the ability to adapt proactively to changing environmental conditions and recover quickly from the negative consequences of external shocks triggered by extreme weather events. This indicates that climate resilient thinking goes beyond but not exclude climate protection or reactive climate adaptation, as described through Walker and Salt's metaphor of a ball in a basin: The ball (i.e., urban system) maintains its general features and functions in a basin (the ability to change or respond to a shock), but after external extreme events, the ball can be pushed into a new basin with different structures and conditions, by maintaining its self-organizing capacity [7]. Responding to an external shock enables a city to recover after extreme events and to keep its basic essential functions, which is also highly depending on the public wellbeing, the build environment and natural capital [8]. As the vulnerability of the exposed people plays a major role in such events, social inequity in health and environmental infrastructure access can even reinforce potential harms through extreme events [9,10]. Environmental justice or social-ecological equity is a social aim to provide adequate access to spatial and environmental goods (including human protection against environmental burdens or security of climate extreme events), which is also affecting the quality of life at a place of residence. Especially subgroups like the elderly, infants, homeless, poor, or disabled tempt to be more vulnerable to environmental burdens, often driven by residential segregation processes over time [11]. To establish a connection, a current issue of social-ecological inequalities and extreme weather events is that "there have been relatively few attempts to integrate environmental justice into resilience thinking", although both domains are inextricably intertwined [12,13]. For urban planners, this demands designing settlements and infrastructures to meet the challenges of today's and tomorrow's climate, while also capturing connections between vulnerabilities and social-environmental challenges [14]. In a sense of a "just climate resilience", risks to the urban system and its subsystems must be examined in a holistic way [8,15]. This requires also a parallel modelling approach which means that demographic and socioeconomic changes are projected in parallel to the changes of the climatic system consideration of socio-economic changes [16]. Over the last 10 years, the number of international publications on resilience in general has increased exponentially, underlining the attraction of the topic [17,18]. This enormous popularity leads to the stimulation of many interdisciplinary dialogues in academic and policy circles [18]. On the contrary, due to the wide-ranging forms of interpretation, this "fuzziness" often causes ambiguities in the scientific operationalization process and therefore impedes convergent decision making for new strategies and policies [19–21]. Fuzzy logic provides a suitable tool for modelling vague, imprecise, incomplete and subjective data, combining linguistic variables with IF-THEN rules in order to emulate human reasoning. Therefore, fuzzy logic is an effective candidate for measuring and assessing resilience, e.g., in Multi Criteria Decision Analyses (MCDA) [22].

Since 2015, there is also a considerable interest of the German Federal Ministry of Education and Research (BMBF) in funding research projects that are dealing with adaptation to climate change and elaborating solutions for cities and regions to strengthen their resilience [23]. The work is part of the BMBF project "Zukunft-Stadt-Region-Ruhr" (ZUKUR), which focuses on a cross-disciplinary approach to contribute to the reduction of social-ecological inequalities and the increase of climate resilience at the scale of regions, cities and neighborhoods. One key research aim of ZUKUR is to find out, whether environmental disadvantaged and sensitive societal groups are extra affected by multiple environmental threads in the Ruhr-Area, Germany. This article demonstrates an interdisciplinary GIS-based fuzzy logic approach on the City of Dortmund to examine spatial distribution patterns in the light of climate resilience and social-ecological disparities. On the basis of a comprehensible framework and via cartographical visualizations, potential (non-)climate resilient locations can be identified. Following this line of thought, the debate on climate resilience indicators and open geodata—especially in Germany—should be enriched. The results should provide a point of departure to launch an evaluation process in order to inform urban planning and decision makers early about climate impacts

and spatial disparities. Doing so, also allows monitoring the progress and effectiveness of devised climate resilience strategies over time.

2. A Brief Review of Understanding and Measuring Climate Resilience

The resilience term initially got popular by the psychologist E. Werner after documenting the individual development of 698 Hawaiian children over 40 years. The major finding was that some children recovered more from similar perinatal traumata and adverse conditions (e.g., poverty) than others. Those children were "resilient" [24]. In 1973, C. S. Holling introduced the resilience concept to the social-ecological sector, describing it as the capacity of an ecosystem to retain its basic organization while undergoing necessary change in the face of ecological disturbances (e.g., by human) [25]. Here, the bounce forward behavior of an ecosystem after a disturbance joined the scientific discourse and replaced previous perspectives on a bounce back effect into equilibrium, [26]. While the global debate around climate change got more serious at the late 1990s, resilience also gained prominence in the field of climate adaptation in cities and regions [27]. Today, the opportunity to innovation and reorganization after disturbances for a city as a normative agenda is raising a multitude of urban planning topics, often following the dynamic credo that "we hardly ever return to where we were" [21]. First influences on European spatial planning can be identified by the fact that climate and disaster risks should be important elements in the decision making process of the environmental impact assessment (EIA) [28]. Climate resilience is also widely understood as a complement to a sustainable development, because the transition towards a state that meets the needs of the present without compromising the ability to meet the future generations is prevented, if climate threats interrupt planning processes [29–31]. As a consequence, policies that promote climate resilience can also contribute to more sustainable structures, not least because resilience is addressed by Sustainable Development Goal 11 (SDG) of the United Nations (UN) 2030 Agenda [32–34].

It is not intended to further expand the theoretical debate of the resilience concept, as this has been conducted thoroughly in previous studies [17,35,36]. Nevertheless, for a comprehensible operationalization and measuring procedure in GIS, a pragmatic definition has to be chosen which shows the key aspects of climate resilience of a city with respect to its social-ecological systems [37]. Drawing on the great amount of existing research articles and reviews, the essential components of climate resilience respected in this study are summarized in Table 1. In theory, the more pronounced these components are, the more resilient a city is to weather related stresses and shocks.

Table 1. Persistent key components of climate resilience definitions respecting different researches.

	Explanation	Source
R	Robustness and adaptiveness to climate related stresses and shocks	[35,38]
E	Evaluation and Monitoring: resilience as a process	[39,40]
S	Scale (Countries, Regions, Cities, Neighborhoods, Individual)	[39–42]
I	Interdisciplinarity: resilience as umbrella for different sectors	[18,40]
L	Learning and innovation	[37,43,44]
I	Information and transparency: resilience as participation tool	[40,45]
E	Environment (natural and built up)	[17,35]
N	Networked systems and actors (multilevel governance)	[35]
C	Capacity to transform after disturbance but maintain self-organization	[7,21,46]
E	Equity and Justice: resilience measurements must not exclude others	[42,44,47,48]

When it comes to the measurement of climate resilience, robustness (Robustness describes the ability of a city (and its subsystems) to withstand external shocks, to absorb them or to limit the adverse effects and consequences) as well as adaptiveness (Adaptiveness enables a city to cope with adverse effects and to respond to changed climatic conditions in the long term, which requires in particular financial resources as well as planning and design decisions [49]) are regarded as the two prerequisites that can be further operationalized, embracing the other aspects mentioned in Table 1 [50,51]. While

robustness can be covered quite well with secondary (geo-)data, the adaptiveness concept is mostly seen through a more qualitative lens and therefore challenging to manage in GIS-based analysis. Currently, this primary data can be assessed by volunteered geographic information (VGI), household surveys or interviews on topics like active climate adaptation strategies and masterplans [45,52]. On the other hand, if not integrated into existing surveys, such primary data collection may be very time and cost consuming. In addition, it is difficult to guarantee a full coverage of an entire city while only catching a brief impression of the interviewees.

From a global point of view, the GIS-based measurement of resilience with indices or scorecards is nothing new [53–57]. Unfortunately, a concrete application in Germany, especially *within* the community scale, is still missing. For example, a first interdisciplinary proposal could be perceived in 2010 by comparing the vulnerability of German autonomous cities and regions using 18 indicators [58]. As a first step onto resilience measurement, Brunetta and Salata conceived a GIS-approach to map the impact of shocks and linear pressures on sensitivities in the city of Moncalieri, Italy [59]. Moghadas et al. introduced a multi criteria approach using weighting factors for assessing urban flood resilience in the 22 urban districts of Tehran, Iran [60]. Based on several workshops and literature review, in 2019 Feldmeyer et al. provided a theoretical framework of 24 indicators to assess urban climate resilience at city scale in Germany [40]. To our knowledge, these indicators have not been applied or tested on a practical example.

To summarize, predefined metrics on climate resilience in Germany are too abstract for urban planning decisions, as the results would not show distributional effects, but one resilience score for the whole urban fabric or its districts, corresponding to the Modifiable Arial Unit Problem (MAUP) [61]. Often, these limitations are influenced by data restrictions. Furthermore, because of the different situations cities are facing, it is difficult to identify if one city is more resilient than the other using the same indicator set. Every municipality is shaped by its own demographic and institutional structures. External shocks may occur in different places, which accordingly implies that "a single prescriptive scorecard does not suit cities of different sizes and contexts" [39].

3. Study Area

The City of Dortmund, which belongs to the federal state of North Rhine-Westphalia (NRW), is located in the Ruhr-Area, the largest urbanized agglomeration in Germany, where the three administrative districts Münster, Düsseldorf, and Arnsberg come together (Figure 1). With about 600,000 inhabitants (2018) and a size of 280 km^2, Dortmund is the largest city in the Ruhr-Area and one of the main economic hubs in NRW [62]. During the phase of industrialization in the 19th century, Dortmund quickly developed into a center of coal and steel industry, which led to an increased immigration of workers from Eastern Europe and the establishment of new workers' housing estates. In the late 20th century, deindustrialization processes resulted in enormous brown fields and a fundamental transition from a heavy-industry based economy to a service sector based model in the whole Ruhr-Area, which was accompanied by high unemployment rates caused by a loss of 90,000 jobs between 1960 and 1994 just in the City of Dortmund [63]. While retaining the image of an industrial city, new jobs were created, mainly in the tertiary and finally quaternary sector. Especially the southern districts of Dortmund now offer attractive housing and employment locations, whereas the northern districts are marked by dense building structures with a high degree of unemployment and migration background, finally resulting in a socioeconomic north-south polarization [64].
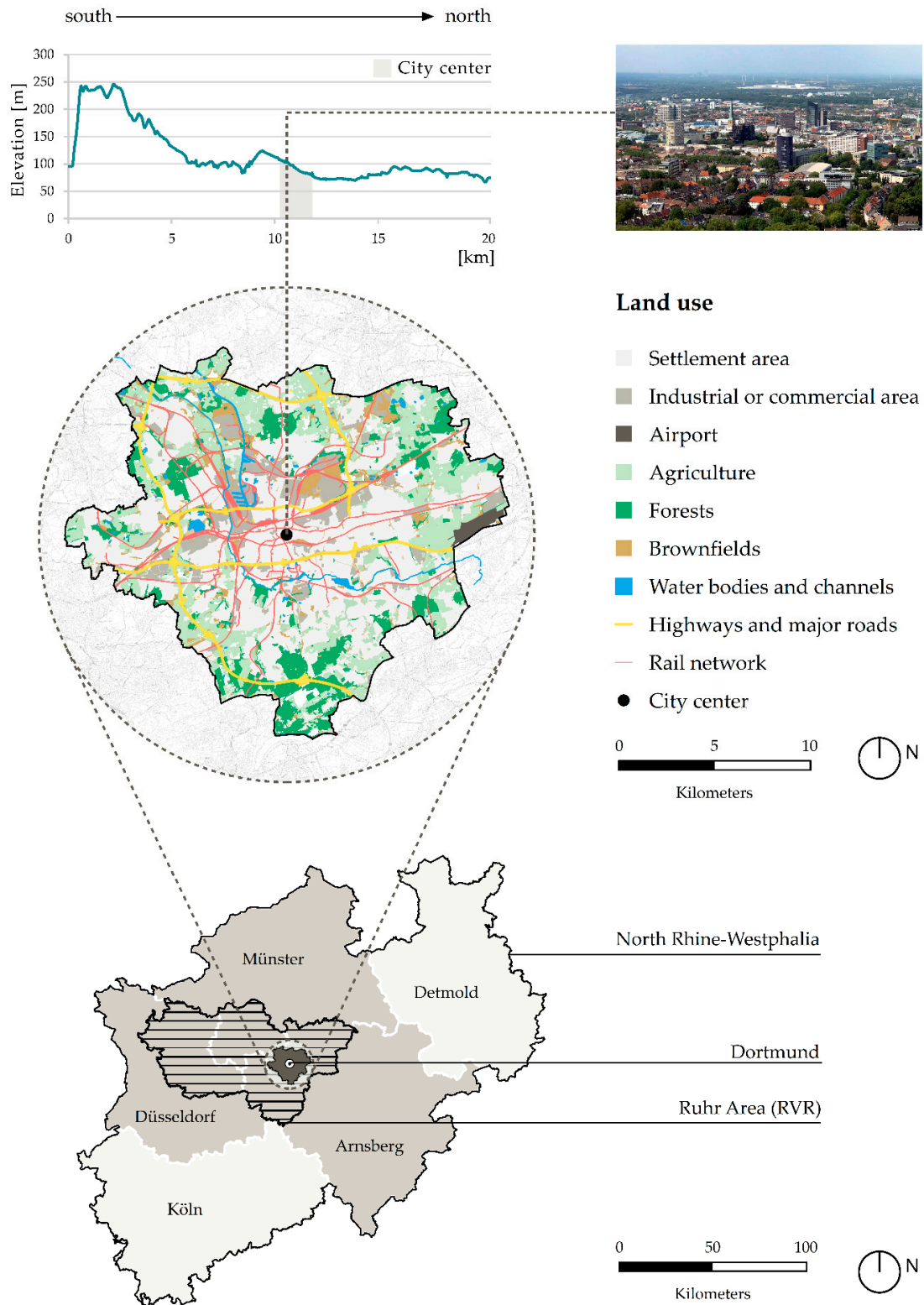
Figure 1. Study area.

Today, as another result of former coal mining activities, large parts of the city's territory are subsided up to 20 m, which are mostly equipped with artificial drainage facilities [65]. The land use of the central city is characterized by a high degree of settlement. Approximately one third of the settlement areas are sealed to more than 60% and often characterized by urban heat islands. On the

contrary, radial surroundings of open and green spaces as well as agricultural uses are providing nightly fresh and cold air.

The two main reasons for choosing the City of Dortmund as study area are as follows:

1. During the last decade, the effects of climate change like urban flooding, storms, heat waves and droughts have been particularly noticeable for local residents. Significantly urban flooding due to a heavy rainfall event in July 2008 caused damage to infrastructures and residential properties: Within two and a half hours, 203 mm of precipitation fell over the western part of Dortmund, especially the sub-districts Marten and Dorstfeld [66].

   The drought and hot summer of 2018 enforced many urban heat islands and crop losses, while storms in 2014, 2018 and 2019 caused damage and harm to people and the built environment. As a reaction to the increasing number of extreme weather events, on 15 November 2018 the council decided to develop an integrated climate adaptation masterplan to strengthen resilience for the entire city. The analysis results could support the conceptualization procedure. Previous GIS-based studies have also shown that—to a certain degree—Dortmund is confronted with social-ecological inequalities [67,68].

2. Since January 2017, the availability of open geodata of the surveying and cadastral administration in NRW has been considerably improved [69]. As a consequence, digital elevation models (DEM), digital landscape models (DLM), noise pollution mappings, climate analyses and high-resolution Digital Orthophotos (DOP) are freely available under the German data license »dl-de/by-2-0«. In this sense, there are fewer formal and financial barriers to the outlined research purpose and more precise analyses up to parcel level are feasible. The City of Dortmund should serve as an illustrative example to present the potential application of this free geodata and to connect those individual data sets thematically.

4. Materials and Methods

In general, the workflow of our methodology can be divided into four analytical steps (Figure 2). The initial preparation phase was important to create an overview of current resilience measurements and the landscape of possible indicators. Based on these findings, dimensions, criteria and indicators representing climate resilience of a city were carried out as a hierarchical framework, integrating practical knowledge for adequate indicator selection and data acquisition that fit the priorities of Dortmund. The preparation and indicator grid calculation was based on ArcGIS for Desktop Advanced 10.4.1 (Environmental Systems Research Institute, ESRI) as well as its Spatial Analyst and Network Analyst extensions. In addition, the freely available landscape analysis program FRAGSTATS 4.27 [70,71] and remote sensing software ENVI 5.4 (Exelis Visual Information Solutions) were applied.
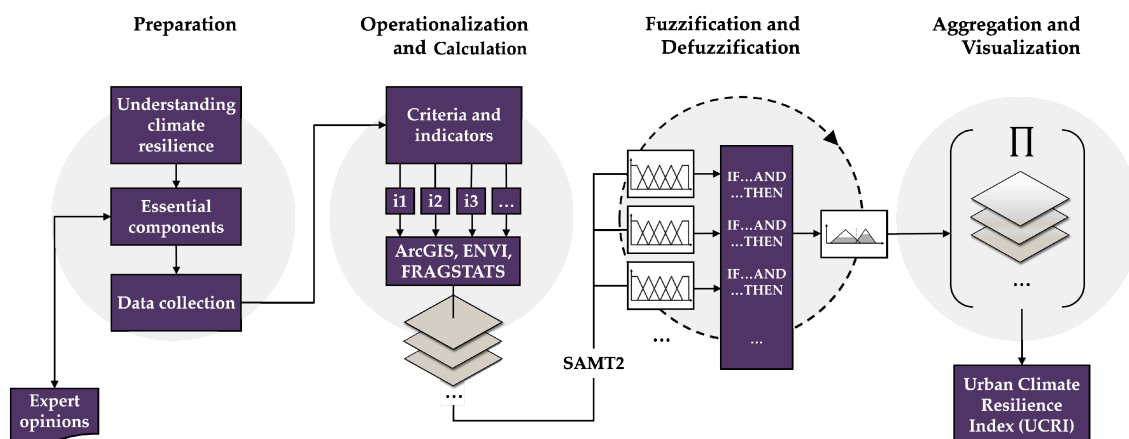

Figure 2. Schematic workflow of the study.

After operationalization and calculation, all raster grids with crisp values were imported into the freely available Spatial Analysis and Modelling Tool SAMT2 [72,73], followed by fuzzification with corresponding linguistic variables, rule-based inference process and defuzzification to standardized crisp variables. This step was iterated on every hierarchical level (indicators, criteria and dimensions) of the framework. The final procedure was the aggregation of the defuzzificated raster grids to a general Urban Climate Resilience Index (UCRI), visualizing more and less climate resilient locations within the community scale.

4.1. Data Collection and Preparation

To properly address the situated problem statement, the use of consistent data is essential. As described earlier, secondary open data that is routinely refreshed and published by statistical agencies is important for a city to compare its own state over time. For this study, a broad dataset was collected, mainly composed of raster, vector and socio-economic data (Table 2). With the use of the freely available road vectors as linear features from OpenStreetMap (OSM), two network datasets both for car driving as well as walking routes were created using Network Analyst. This procedure allowed us to quantify the access of different locations within a certain catchment area (i.e., the access of open and green spaces) in a more realistic way than other tools like simple buffering or Euclidean distance, because it orientates on the real road network like a navigation system [74]. For car driving, missing information on maxspeed limitations (km/h) were subsequently added, using standard values for each road type (Table A1) [75]. Fire brigade operations due to extreme weather events (storms, heavy rainfalls and heat stress) between 2008 and 2018 were provided as table-based long–lat-coordinates, which initially were converted to multipoint data in GIS. Raster data on noise pollution was previously modelled by the Environmental Office Dortmund. Other noise pollutants like construction noise or sports and recreational noise are not included.

Yet important questions about social-ecological phenomena and data on air pollution were not included in this work, as the finest available spatial resolution here is 1×1 km of different pollutant emissions in NRW for 2013 and thus too coarse and outdated for the research purpose. However, because noise pollution is likely to spatially correlate on air pollution (especially next to streets and industrial sites), the noise pollution mapping appears to give an insight, where potential air pollution could occur within the city [76]. The provided heavy rain hazard mapping was previously modelled by the engineering office Beck GmbH & Co. KG (City of Wuppertal) using a DSM of 2012 for a return period of 100 years on a spatial resolution of 1×1 m. The mapping consists of three raster images, including flow directions, water depths in m and flow velocity in m/s. Unfortunately, a modelling of a return period of more than 200 years, which happened in Dortmund Marten in 2008, was not available. Cold air volume flows in m^3/s have been calculated in 2012 by GEO-NET Umweltconsulting GmbH in cooperation with Prof. Dr. G. Groß (University Hannover) for entire NRW with the application of the mesoscale FITNAH climate simulation model, respecting the development of various climatic parameters such as wind and temperature over a daily cycle on a grid of 100×100 m. For spatial modelling, an air temperature of 20 °C at 21 o'clock, a cloudless sky and no supra-regional wind currents for modelling was assumed. In order to generate a digital surface and digital terrain model, Airborne Laserscanning 3D- point data with a 0.5 m interval was interpolated to a 1×1 m raster using natural neighbor algorithm in GIS. By subtracting the DTM of the DSM, a normalized Digital Surface Model (nDSM) could be calculated, highlighting off-terrain objects (e.g., buildings, trees etc.). Building parcels of the city with actual land use could be examined and extracted out of the Authoritative real estate cadastre information system (ALKIS). The Land Use classification of the ATKIS Basic DLM meets the requirements for high thematic and spatial resolution (±3 m), while being available for complete NRW with a nationwide thematically consistency and a cyclically update every 3–5 years.

Table 2. Data used.

Format	Description	Resolution/Scale	Source	Year
Raster	Landsat 8 Satellite Image (path 197/row 24)	30 × 30 m (Cloud Cover: 5.22%)	United States Geological Survey (USGS)	2018
	Digital Orthophotos (n = 332)	0.01 × 0.01 m	Geobasis NRW (dl-de/by-2-0)	2018
	Heavy rain hazard mapping (return period 1%/year)	1 × 1 m	Municipal Drainage Office Dortmund	2019
	Noise mapping from different sources (trains, trams, roads, industry)	10 × 10 m	Environmental Office Dortmund; Federal Office for Railways Bonn	2018
	Digital terrain model (DTM) and digital surface model (DSM)	Point data with 0.5 m spacing	Geobasis NRW (dl-de/by-2-0)	2018
Vector	Land Use, Digital Landscape Model of the Federal topographic information system (ATKIS Basis-DLM)	1:10.000	Geobasis NRW (dl-de/by-2-0)	2019
	Building parcels with land use information, Authoritative real estate cadastre information system (ALKIS)	Parcel Level	GeobasisNRW (dl-de/by-2-0)	2019
	Points of Interest (POI)	Parcel Level	City of Dortmund Website	2019
	Road Network	Parcel Level	OpenStreetMap (Geofabrik GmbH, www.download.geofabrik.de)	2019
	Fire brigade operations due to extreme weather events	Long/Lat Coordinates	Institute of Fire Service and Rescue Technology (IFR) Dortmund	2008–2018
	Volume of cold-air flow in m^3/s	100 × 100 m	NRW Office for the Protection of Nature, the Environment and Consumers (LANUV)	2019
Socio-demo-graphic and -Economic data	Proportion of infants (0–11 years)	Statistical sub-districts (n = 170)	Statistics Office Dortmund	2017
	Proportion of elderly +65 years			
	Proportion of SGBII and SGB XII recipients			
	Proportion of single households			
Digital Land Use Plans	Official preparatory Land Use Plan	1:20.000	City of Dortmund Website	2004
	Land Use plans Ev148, InN222, Hu144	Parcel Level		2014, 2012, 1985
	Climate mitigation measures	1:500		Unk.
			Freely available	On demand

Descriptive statistics on unemployment benefit recipients according to the second and twelfth book of the Code of Social Law (SGBII and SGBXII) as well as demographic structure were also involved to this study. They represent potential vulnerable groups which are likely to be particularly exposed to extreme weather events and its consequences, including injuries, heat stress or premature death. Additional information of land use plans and measurements have been manually digitalized in order to capture areas where climate resilience related projects are located in Dortmund.

During the pre-processing of the single Landsat satellite image, Dark Object Subtraction (DOS) algorithm was used to remove atmospheric scattering effects like dust and haze [77]. The transformation to reflectance values is an automated process in ENVI 5.4 by using the sourced Landsat metadata. Cloudless and georectified DOPs, recorded on 29 June 2018, are distributed in a 1 × 1 km square-grid, which had to be mosaicked for the entire study area in order to enable further remote sensing analysis.

Finally, all geodata was projected into the Universal Transverse Mercator coordinate system (UTM) zone 32 north and clipped to the study area, except the two network datasets, which additionally extended 5 km around the city border in order to integrate connections from adjacent municipalities. We chose a consistent 10 × 10 m raster analysis unit, as it provides a high level of detail and compromises between computing time and feasibility. Each cell is finally representing an area which will be tested amongst criteria and indicators for a climate resilient city.

4.2. Indicator Selection and Calculation

In order to coordinate and specify which external stressors and social sensitivities are prioritized for Dortmund, preliminary expert interviews with two staff members of Dortmund's urban planning and environmental office were assessed. Based on the findings of Meerow et al., the following three questions have been asked [12,35]:

1.   Whose resilience is prioritized?
2.   What climate related extreme events should Dortmund be resilient to?
3.   Is the resilience of some areas prioritized over others?

To summarize the experts' answers, major sensitive groups are inhabitants with lower income, as they are living in more densely populated neighborhoods and self-protection as well as personal provision are limited in monetary terms. Heavy rainfall events, air pollution of industrial sites and urban heat island effects are important stressors for Dortmund, while green and open spaces are important as resilience strengthening areas. These findings were taken into account for further indicator selection.

The indicator selection depended on the possibility to be calculated in GIS with the gathered data and therefore matching the fine scale up to neighborhood level. Furthermore, a clear relevance to climate resilience based on the essentials presented in Section 2 had to be ensured. For a better understanding about the framework, criteria and indicators can be structured to an overarching objective in a hierarchical fashion, also referred to as "granulation" in fuzzy logic analyses [78]. In our case, climate resilience of a certain areal (here: 10×10 m pixel) within the city corresponds to a normatively overall objective. The maximum number of three raster-grids is allowed as input in SAMT2, so that not more than three factors can be considered on each hierarchical step. Due to the chosen analysis scale and corresponding data restrictions, many indicators which previously were set up for cities do not fit to our purpose, e.g., percent population with a vehicle or percent population with health insurance coverage [20]. On the other hand, the creation and calculation of new indicators on a much finer scale may allow to unmask interdependencies between empirical data that is recorded on broader scales.

As climate resilience is widely seen as a holistic approach, the urban system as a whole firstly had to be operationalized into its major subsystems. Following the general classification of Feldmeyer et al. [40] and Cutter et al. [37], initially five dimensions of an urban system (Environment, Society, Infrastructure, Economy, and Institution) were set up as starting point for operationalization (Table 3). An important precondition was to include social-ecological factors into the indicator set, as the public wellbeing and health of the society plays a major role in terms of the robustness of the system. As a consequence, these factors are particularly present in the Environment (resources and burdens) and Society dimensions. As pointed out in Section 2, the dimensions Environment, Society, and Infrastructure refer to the robustness of the system, while Economy and Institution correspond to its adaptiveness. Of course, this assignment is arguable, but if a city has no prospering economy and political willingness for adaptation measurements—including the repairs of local damages by weather extremes—the adaptiveness may be less pronounced. To describe climate resilience phenomena for all five dimensions, 18 indicators belonging to 12 criteria were determined which will be explained in the following sections.

Table 3. Final indicator set for measuring climate resilience in Dortmund.

Dimension	Criterion	Indicator (GIS-Acronym)	Source
Robustness			
Environment	Retention sites	Degree of unsealed ground (DUG)	[40]
		Slope (SL)	[79]
	Resources	Accessibility of public open and green spaces (AccG)	[42,67,80]
		Ventilation status (VS)	[40,81]
	Burdens	Heat stress (PET)	[82]
		Noise pollution (NP)	[67]
Society	Hazard to housing	Potentially flooded housing parcels (HFld)	[59]
	History of extreme events	Number of fire brigade operations due to extreme weather events (2008–2018) (NFO)	[40]
	Demographic structure	Number of 0–11 years olds (INF)	[68,83]
		Number of +65 years olds (ELD)	[67,83]
		Number of single-households (SHH)	[83,84]
Infrastructure	Hazard to Critical Infrastructures	Potentially flooded technical and social infrastructures (TSFld)	[59,83]
		Potentially flooded transport and traffic infrastructures (TTFld)	[59,83]
	Civil Protection	Accessibility by fire brigade (AccF)	[85]
	Health access	Drive time to hospitals (AccH)	[86]
Adaptiveness			
Economy	Diversity of business	Shannon Diversity Index (SHDI)	[40]
	Unemployment	Number of SGBII and SGBXII recipients (SGB)	[20]
Institution	Strategies and plans	Implementation status of climate resilience related measurements, research projects and land use plans (IN)	[37,40,87]

4.2.1. Environment

Unsealed surfaces play a major role as natural infiltration site in case of heavy rainfalls. The Normalized Difference Vegetation Index (NDVI) is a multidisciplinary remote sensing index for i.e., determining and analyzing healthy green vegetation, vegetation recovery after a fire occurrence, or urban flooding [88]. As one of the most popular indices in remote sensing, it is simply and quickly to assess with almost every multispectral imagery in GIS, as long as a nearinfrared (NIR) and red (R) band is included:

$$NDVI = \frac{NIR - R}{NIR + R} \tag{1}$$

The DOP-mosaic with NIR band was used to calculate the NDVI, whereby the resulting values ranged between −1 (water), 0 (bare soil) and +1 (trees, healthy vegetation). After visual inspection, a threshold of 0 was set for unsealed surface extraction, including agricultural uses and bare soils. As water is also representing an unsealed surface, an extraction threshold was set on −0.95. The degree of unsealed ground was derived by utilizing moving window technique in FRAGSTATS with a window size of 100 m, because at this stage first variations in land use were visually pointed out in the study area. As slopes are increasing, surface water run-off tends to cause erosion on land cover, so it was also important to respect terrain characteristics for heavy rainfall events. Therefore, the generation of slopes as degree levels in GIS with the high resolution DTM finally quantified the second complementary indicator for retention sites. A detailed analysis of the local sewer system may be an important factor

too, but would go beyond the scope of this paper. The classification corresponds to (0°–2°, flat), (3°–6°, slowly), (7°–15°, oblique), (16°–25°, steep), and (>25°, very steep) conditions.

The influence on public health of urban green spaces has become an increasingly important topic for many municipalities, as urban green spaces tend to have direct and indirect positive contributions to the psychological, mental and social wellbeing. Furthermore, they also have a compensatory function with regard to noise pollution or climatic extremes, offer opportunities for social contacts and an incentive for physical activities. Open and green spaces like forests, urban parks and cemeteries with a size of ≥1 ha were extracted from the ATKIS dataset, respecting the accessibility to the general public which led to the exclusion of land containing private allotments. For a proper network analysis, entrances as point data have been assessed by intersecting the perimeters of open and green spaces with the footway line network created out of the OSM dataset [89]. With the performance of an Origin/Destination (OD) Cost-Matrix in Network Analyst, minimum distances from every point (Origins) in Dortmund to the closest entrances (Destinations) were modelled. Meters were chosen as impedance, because walking speed strongly depends on individual conditions. The thresholds are (0–250 m, very close), (250–500 m, close), (500–750 m, moderate), (750–1000 m, far), (>1000 m, very far) [80]. In addition, to create a transitional raster grid for air status in the city, the point data of cold-air flow in m³/s was interpolated using Inverse Distance Weighting (IDW) method and classified according to the LANUV categorization (>300–1500 m³/s, moderate), (>1500–2700 m³/s, high), (>2700 m³/s, very high).

By confronting the status quo with reference cases that already took place in the real world, a more realistic picture of climate resilience can be drawn. Correspondingly, in order to detect regions with heat stress potential, land surface temperatures (LST) have been derived with band 10 (Thermal Infrared) of the Landsat 8 satellite image on a hot summer day in 2018. After image calibration for band 10, at-satellite brightness temperature (T_B) in °C was calculated:

$$T_B = \frac{K_2}{\ln\left(\frac{K_1}{L_\lambda} + 1\right)} - 273.15 \tag{2}$$

K1 (774.8853) and *K2* (1321.0789) are channel-specific coefficients which can be retrieved from the supplied metadata, while L_λ is at-sensor spectral radiance of band 10. T_B illustrates a theoretical value which has to be further adjusted by spectral emissivity (ε) [90]. The value of ε can be derived from existing literature:

$$\varepsilon = \varepsilon_v * P_v + \varepsilon_s * (1 - P_v) \tag{3}$$

whereby ε_v is the in situ emissivity of vegetation, ε_s is the emissivity of bare soils and P_v is the ratio of vegetation and bare soils [91]. The value for ε_v corresponds to 0.973 and for ε_s 0.966 when using Band 10 of a Landsat 8 scene [92]. P_v can be calculated with the NDVI, which is to be retrieved from Landsat 8 NIR and R bands:

$$P_v = \left(\frac{NDVI - NDVI_{MIN}}{NDVI_{MAX} - NDVI_{MIN}} \right)^2 \tag{4}$$

$NDVI_{MIN}$ represents the threshold for bare soil and $NDVI_{MAX}$ the threshold where green vegetation occurs. A value of 0.2 was set for $NDVI_{MIN}$ and 0.5 for $NDVI_{MAX}$ [93]. After retrieving ε and P_v, the calculation of LST, represented by T_s, according to Boltzmann's law was retrieved as follows:

$$T_s = \frac{1}{\varepsilon^{1/4}} * T_B \tag{5}$$

Krüger et al. conceived a linear correlation (r = 0.735) between LST of Landsat imagery and the measured physiological equivalent temperature (*PET*) in the German City of Dresden [82]. As a result, the formula for transforming LST into estimated PET values is as follows:

$$PET = 17.077 + 0.465 * LST \tag{6}$$

We applied this formula to our calculated LST values, totally aware of the fact that Dortmund may be confronted with other environmental conditions as Dresden, but both cities are located in Germany, share a similar size in population as well as administrative area and lie on almost the same latitude. The final PET-thresholds were set as (18–23 °C, no thermal stress), (23–29 °C, slight heat stress), (29–35 °C, moderate heat stress), (35–41 °C, strong heat stress) and (>41 °C, extreme heat stress). The same thresholds have been used in a previous study [94]. As another environmental stressor, noise pollution was considered in our analysis, because high noise level exposures have adversely effects on the public wellbeing [95]. For the noise pollution indicator, the three input raster datasets on different noise pollutants have undergone a logarithmic aggregation in GIS, resulting in a 10 × 10 m raster image on a day-evening-night level (L_{DEN}) in decibels (dB). High noise levels are defined as noise levels above 55 dB on L_{DEN}, so the final classification was set as (10–25 dB, very quiet), (25–40 dB, quiet), (40–55 dB, moderate), (55–70 dB, loud), (>70 dB, very loud) [96].

4.2.2. Society

As heavy rainfall events are a crucial issue for the City of Dortmund, flood hazard rating (*HR*) was carried out with the heavy rainfall raster images in GIS, using the following formula of DEFRA, which was also applied for a flood risk assessment in Spain [97]:

$$HR = h\,(v + 0.5) + df \tag{7}$$

Whereby *h* represents flood depth in m, *v* velocity in m/s and *df* the debris factor, ranging between 0 and 1 depending on flood depths, velocities and dominant land uses. There is a low hazard if *HR* < 0.75, danger for some if 0.75 < *HR* < 1.5, danger for most if 1.5 < *HR* < 2.5 and danger for all if *HR* > 2.5 [98].

We chose infants and small children (0 to 11 years), the elderly (+65 years) and single households as sensitive population groups who are particularly prone to extreme weather events, because they tend to have less physical or personal abilities to flee from water or to cope with heat stress, while also being unable to reach safety for themselves [83]. Assuming an average storey height of 3.35 m in Dortmund [99], with the use of the building footprints of the ALKIS dataset and the nDSM, average heights of each building with residential or mixed land use could be automatically extracted and rescaled to story numbers. Concerning the resulted story numbers and the demographic data on sub-district level, we applied a dasymetric mapping method to disaggregate population subgroups onto a pixel size of 10 × 10 m:

$$P = \frac{(R_n A_n) * N}{E} \tag{8}$$

where *P* is the number of people within a pixel, R_n is the relative density of the mapping unit population with land-cover type A. A_n is the area of mapping unit. *N* is the actual population of each statistical sub-district. *E* is the expected population of enumeration unit calculated using relative densities. *E* equals the sum of the products of relative density and the proportion of each land-cover type in each enumeration unit [100,101]. Drawing on a previous study on Dortmund which contained expert knowledge about relative density values for four land cover classes, we assigned the same weightings for apportioning the sub-district related data [67]:

1. residential use, up to two storeys: 15%,
2. residential use, three to five storeys: 30%,
3. residential use, more than five storeys: 40%, and
4. residential mixed use: 15%.

Consequently, all uninhabited areas (agriculture, forests, water etc.) were reclassified to a value of 0. After the disaggregating process for each subgroup, the synthetic population estimations were standardized to equal intervalled z-scores as standard deviations from mean to point out hotspot

locations. Besides the spatial population sensitivity identification, it was also important to map chains of effects, where climate related extreme events occurred in the past and led to physical damages or helplessness for local residents. In order to calculate the density of fire brigade events of the last decade, we initially used the incremental Moran's I tool in ArcGIS to evaluate an appropriate search radius for density mapping. This procedure allows to inform the user whether the spatial pattern of a set of points is grouped or random by gradually increasing the search radius. If the results show a statistical significance at a certain search distance, a positive Moran's I index value indicates a tendency to clustering. Setting a search distance of 2400 m as clustering threshold, the final kernel raster grid was created. Five equal intervals concerning standard deviation from mean were created for classification.

4.2.3. Infrastructure

Critical infrastructures are organizations or institutions of special importance to society (i.e., transportation, energy and water supply, emergency services etc.). In the event of a failure or functional impairments, it would lead to significant disturbances of social life and public safety as well as to negative cascade effects [102]. Following the categorization of the German Federal Ministry of the Interior (BMI), technical and social infrastructure as well as traffic and road infrastructure (Table A2) have been extracted by the corresponding codes from the ALKIS dataset and masked out of the HR-raster image. This procedure allowed us to identify hazard related infrastructures.

Enhancing the spatial and time-based accessibility of fire services is important to improve emergency response, minimize property loss as well as to reduce injuries and deaths [85]. Fire brigades (including volunteers) were extracted from the POI dataset. Drive time in minutes outgoing from fire brigade locations to every point in Dortmund was calculated with an OD Cost Matrix for vehicle driving network dataset. In the event of an emergency call, fire brigades have free access on roads, so that no barriers or restrictions (e.g., traffic lights or one way roads) in the network dataset were taken into account. The fire brigade should arrive at the place of hazard within 8 min after emergency call in order to be able to carry out human rescues still in time [103]. Therefore, the final classification of drive time was set as (≤4 min, very quick), (>4–8 min, quick), (8–12 min, moderate), (12–16 min rather late), (>16 min, late).

By using the same network dataset, hospital locations in Dortmund were extracted by the POI dataset, followed by the calculation of drive time in minutes from every location in Dortmund with the max speed and the length of each line segment as variables. We classified the results into five equal intervals, ranging from (0–3 min, very fast), (3–6 min, fast), (6–9 min, moderate), (9–12 min, far), and (>12 min, very far).

4.2.4. Economy

The economic attractiveness of a city is a crucial factor for new companies. Cities with a high diversity of businesses across multiple sectors tend to ensure a more pronounced adaptability and faster recovery from external shocks, since there are more opportunities to provide social services and cultural programs. Furthermore, diversity enhances flexibility for different working fields and helps to diminish segregation processes (functional and social), which also corresponds to the equity component in resilience debates [104]. To assess business diversity, Shannon Diversity Index (SHDI) with 1 km square-width (A search radius of 1 km indicated clustering effects of the dataset after incremental Moran's I calculation.) moving window technique was calculated for each pixel in FRAGSTATS by using ALKIS building footprints excluding residential areas and uninhabited objects like transformer stations or garages as potential workplaces:

$$SHDI = -\sum_{i=1}^{m} (P_i * \ln P_i) \tag{9}$$

P_i is the proportion of the landscape occupied by patch class *i*. *SHDI* assumes values above 0, without upper limit, while *SHDI* = 0 (no diversity) when the regarded sample only contains one land use [70]. If the amount of different patch types (richness) increases and/or the proportional distribution of area among patch types becomes more even (evenness), *SHDI* increases simultaneously. Because there is no reference value to compare with, we standardized the *SHDI* values to standard deviations from mean and created five equal intervals for classification.

As pointed out in the expert interviews, unemployed people tend to have less monetary resources to adapt to climate risks. Therefore, the number SGBII and SGBXII recipients as indicator of unemployment was undergone the same dasymetric mapping procedure and z-standardization as the three indicators for sociodemographic structure in the society dimension.

4.2.5. Institution

In order to create a better understanding about climate mitigation and resilience strengthening strategies, it is important to establish an overview about where and what measurements have been decided so far. The institutional aspect is only represented by one indicator, since it is difficult to capture qualitative adaptation targets in a quantitative manner. However, it is possible to map and rank decisions and measurements on climate resilience and adaptation to visualize their current allocation in an administrative area [105]. Considering theoretical questionnaires on a previous resilience study in Germany [50], official land use plans, research projects and climate adaptation measurements were assessed for the entire city and classified ordinal from 1 (worst) to 5 (best) with regard to their implementation status as follows:

1. No climate adaptation measurements are planned
2. Climate adaptation measurements will be planned
3. Climate adaptation measurements are planned, but not started yet to implement
4. Climate adaptation measurements are currently being tested or implemented
5. Climate adaptation measurements have been implemented (e.g., official land use plan is in force or plan approval procedure is finished)

4.3. Fuzzy Logic Analysis

Although many researches have been undergone in the last decade, climate resilience still contains a lot of vagueness and complexity in its definition. Between the derived thresholds presented in Section 4.2, there are smooth transitions which calls for adequate spatial modelling techniques that respect uncertainties in a multi criteria decision making process [49]. In this work, SAMT2 was used for fuzzy modelling, which is completely programmed in python, so it is applicable on most computer systems.

4.3.1. Fuzzification

Fuzzy logic results are ranging between 0 and 1 as intermediate values between concrete evaluations [106]. In order to convert raw crisp indicator values into fuzzy sets, it is to be determined, to which degree each indicator value belongs to a certain property (degree of membership) using linguistic variables, e.g., in case of PET values, "slight heat stress", "moderate heat stress", and "strong heat stress". Trapezoidal and triangular membership functions are the most commonly used linear types in the fuzzification process and easy to apply in SAMT2. The peak points of triangular or trapezoidal functions are representing a definite membership (thresholds) and vice versa. An overlap between the membership functions is desirable in order to allow smooth transitions between the ranges of indicator values. If information about indicator thresholds are limited, e.g., triangular membership function should be used [107]. A graphical illustration of the used membership functions and thresholds for each indicator grid can be obtained in Figure A1.

4.3.2. Indicator Combination and Inference Method

For each crisp value of a variable, the degree of membership of the associated fuzzy set is checked with IF-THEN-rules. In the THEN-part of the rule, an assignment is made to the output variable as a fuzzy set. The default rule for conclusion finding (fuzzy singleton) in SAMT2 is based on IF X AND Y THEN Z. The AND operator is widely used as premise in a fuzzy rule-based evaluation. Five linguistic terms correspond to 125 (5^3) inference rules to set up for with three indicator grids, which explains why not more than three indicators should be concerned per criterion [108]. After defining rules with membership functions and linguistic variables, singletons were created, where truth membership values are transformed into fuzzy sets with values ranging between 0 and 1. For instance, one rule in SAMT2 was defined as follows:

IF (raster value of indicator PET is {no thermal stress ∨ slight heat stress ∨ moderate heat stress ∨ strong heat stress ∨ extreme heat stress} regarding climate resilience) AND

IF (raster value of indicator NP is {very quiet ∨ quiet ∨ moderate ∨ loud ∨ very loud} regarding climate resilience) THEN

(raster value of environmental burdens is {more robust ∨ rather more robust ∨ moderate robust ∨ rather less robust ∨ less robust}.

All fuzzy sets were transformed using MAX-PROD inference method. We chose an equally weighting for all indicators, because methods for determining weights like the Analytic Hierarchy Process (AHP) by Thomas L. Saaty are always somewhat subjective and do not necessarily reflect real priorities [109]. Furthermore, the use of 18 indicators makes it difficult and time-consuming for experts to significantly allocate different weights, as the more indicators are concerned, no well-defined priorities can be figured out. Finally, relative importance on indicators vary between sectors and over time as local foci are permanently changing [110].

4.3.3. Defuzzification

The last step in fuzzy logic analysis is to transform the cumulated fuzzy inference results back into a crisp set in order to perform further analyses in GIS. In other words, a single-valued output had to be calculated as the best representative within the aggregated fuzzy sets. In SAMT2, the center of gravity (COG) technique is automatically modelled, which can be stated as the weighted sum of the results:

$$x^* = \frac{\sum_x \mu(x)x}{\sum_x \mu(x)} \tag{10}$$

whereby x^* indicates the defuzzified crisp value ranging between 0 and 1, and $\mu(x)$ the output membership function of the output variable x (fuzzy singleton).

4.4. Compromise Programming and Sensitivity Analysis

The use of fuzzy membership functions inhibits a high sensitivity on the resulting maps. Therefore, the reliability and usability of the method had to be examined by comparing fuzzy logic results with a traditional crisp value-based MCDA method. Compromise Programming (CP), a multi-attributive decision method proposed by M. Zeleny [111], is based on the assumption that the achievement of an overall objective (e.g., climate resilience) lays in the nature of human and that the best compromise solution is considered to be given when it is as close as possible to the ideal state. To put it in a mathematical way, an alternative (here: pixel value) measured by several indicators is suitable as a compromise solution, if:

$$L_p(W) = \left[\sum_{j=0}^{n} W_j^p \left| \frac{Z_j^* - Z_j(x)}{Z_j^* - Z_{*j}} \right|^p \right]^{1/p} \rightarrow min \tag{11}$$

whereby Wj ($Wj > 0$, $W_1 + W_2 + \ldots + W_n = 1$) is the individual weight of each indicator (in this work all weightings are equal). Therefore, $L_p(W)$ reflects the weighted distance of each alternative to the ideal

point Z_j^* (here: 1). The more L_p (W) reaches towards 0 ($\rightarrow min$), the closer the alternative to climate resilient and vice versa. Given a natural value of ≥ 1, p is expressed as the degree of compensation and is used to weigh the discrepancy between the ideal point and the real value of an indicator $Z_j(x)$. If $p = 1$, a City-Block-Norm exists, in which worse rated indicator values can be fully compensated by better rated values. The Maximum-Norm with $p = \infty$ represents the opposite (no compensation). In case of $1 < p < \infty$, the Euclidean-Norm with partial compensation applies. Since p is directly influencing the compromise solution, we applied the CP formula for our normalized crisp valued indicator set respecting each Norm in ArcGIS in order to investigate potential driving forces on the decision analysis [90]. We reclassified our normalized indicator grids into five equal classes between 0 and 1, corresponding to less resilient (0.0–0.2), rather less resilient (0.2–0.4), moderate resilient (0.4–0.6), rather more resilient (0.6–0.8) and more resilient (0.8–1.0) [20]. Consequently, the fuzzy logic result was statistically compared to the three results of CP.

5. Results

5.1. Mapping the Subsystems

After the defuzzification processes for every hierarchical step, initially five maps have been obtained, representing the five dimensions of the indicator set. Figure 3 illustrates the interdisciplinarity as well as the diverging foci of resilience. It is plausible that in case of environmental robustness, open and green spaces with high ventilation status, proper accessibility and low sealing are rated higher (blue) than industrial sites or major traffic roads (red). Especially industrial sites are sealed to a high degree and make the highest land surface temperatures (>40 °C) measured by Landsat 8 in the study area. On the other hand, existing forests in the south are partially environmental affected by crossing major roads or not suitable to serve as natural retention sites due to steep slopes. On the societal component, two fire brigade operation hotspots tempt to cluster in the center and the west. The western hotspot is a result of the destructive heavy rain event in Dortmund Marten and Dorstfeld sub-districts, while the city center is also an area of numerous extreme weather related operations in the past. The northern sub-districts surrounding the city center are home to a large amount of infants and children, whereas the southern and eastern suburban districts are more represented by the elderly. Single households are mostly concentrated in the urban core. Regarding infrastructural resilience, it becomes clear that especially the northern edge is less spatially connected to nearby hospitals or fire brigades than the rest of the territory. From the economical adaptiveness point of view, Figure 3 indicates that Dortmund tends to have multiple centers varying in size with a high diversity or evenness throughout the administrative area. However, most of these accumulations are located in the center and the south, whereas the northern part is more influenced by large logistics and industrial sites. In addition, the northern central sub-districts are characterized by a high degree of unemployment. Because the entire city will be regarded for the development of an integrated masterplan on climate adaptation, no raster value was rated worst in the institutional adaptiveness section. However, throughout the city, several climate adaptation or resilience research projects, land use plans and measurements could be carried out. For instance, the sub-districts Dortmund Marten, Nordstadt and Huckarde are currently sceneries for social living labs aiming to increase climate resilience and reduce social and ecological inequalities. Generally speaking, there is a shift in favor of the societal and infrastructural dimension, whereas the institutional, environmental and economical dimensions seem to be less pronounced in the study area. Nevertheless, each dimension is concurring with each other, e.g., if there are more natural areas, which are important for cold air production, recreation and biodiversity, the business diversity is automatically shrinking.
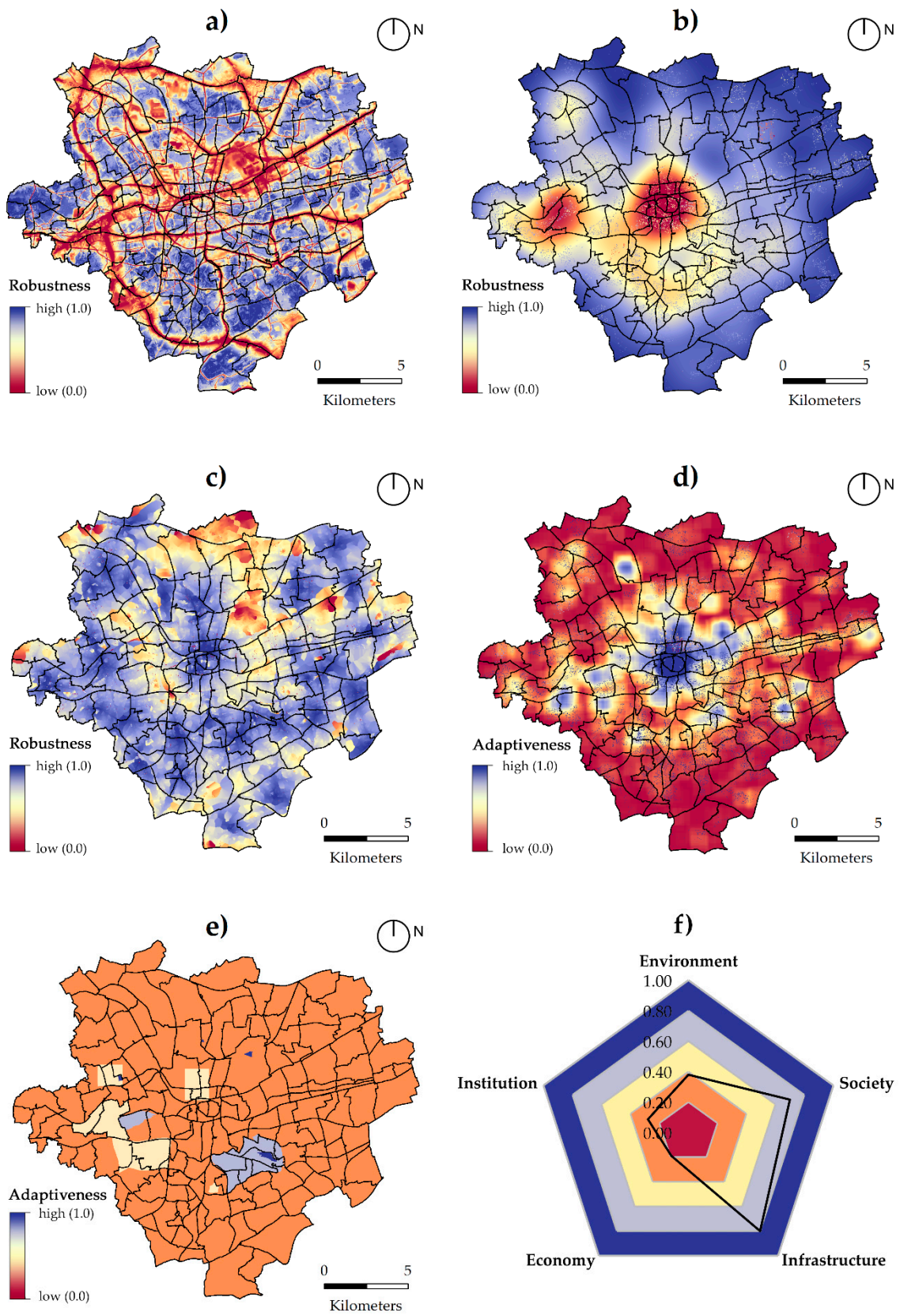
Figure 3. Fuzzy analysis results for the five dimensions, (**a**) environment, (**b**) society, (**c**) infrastructure, (**d**) economy, (**e**) institution, (**f**) comparison of mean values in the study area.

5.2. Urban Climate Resilience Index (UCRI)

Figure 4 presents a five staged rating of the final result in the study area after fuzzy logic application. To follow the spirit of the fuzzy concept, there is no distinct linguistic determination of the resilient area, which is why we chose equally sized classes as z-scores for the visual Urban Climate Resilience Index (UCRI) interpretation. The majority of the calculated pixel values demonstrate moderate or rather more resilient levels, which accounts for the compensation and competing effects between the thematically diverging indicators and dimensions. In addition, there is a tendency that more resilient areas are located outside the urban core, while less resilient land uses like major roads, rail networks and overheated industrial sites are scattered throughout the entire study area. In the urban core (especially the north), a moderate accessibility to green areas, high PET values and soil sealings, low ventilation status, high proportions of single households and unemployment result in rather less climate resilience. The negative influence of fire brigade operations in the last decade stays persistent also in the aggregation of all indicators and become particularly noticeable in the west and the center. Environmental burdens are also a crucial factor for the analysis results, as noise pollution or heat stress will not be perceived less annoying through a good accessibility to public open and green spaces. In general, unsealed areas like forests and lakes in the rural parts of the city tend to be more robust regarding the environmental dimension, while urbanized clusters and industrial sites are rated worse.

Figure 5 shows the UCRI in a more detailed way by comparing the three sub-districts Dortmund Marten, Dortmund Hörde and Clarenberg. It becomes noticeable that the sub-districts vary in population conditions and their environmental states. While in Dortmund Marten the environment is ranked as rather less resilient because of high noise pollution due to highways and interregional railways, the major environment in Hörde and Clarenberg is rated more resilient. Established on a former steelworks areal, the artificial lake Phoenix in Hörde represents a public green and open space as well as a climate adaptation measure, as it serves as a potential retention basin of the adjacent Emscher tributary. Furthermore, the district of Hörde is subject to climate adaptation measurements, which ends up in a high resilient rating of the UCRI. On the other hand, although there seems to be an adequate accessibility to public green and open spaces (e.g., lake phoenix), residential areas in the south (Clarenberg) may not be able to adapt or be robust against climate extreme events due to monetary or physical conditions, which implies that issues on climate resilience are taking place on different dimensions within the urban system.

5.3. Sensitivity Analysis

With regard to Figure 6, the environmental and societal dimensions tend to act as dominant driving factors for the UCRI. The increase of p values results in a decrease of standard deviation, although the Maximum-Norm ($p = 10$) reveals some disparities in the worst class assignments (less resilient). In our fuzzy analysis, the environmental dimension was regarded with no compensation between the indicators, because people won't feel less burdened in a very hot but quiet environment. This fact explains why on the City-Block-Norm and Euclidean-Norm of the CP-method streets and rail networks are rated much higher due to full compensation. In conclusion, the fuzzy logic results may range between the Euclidean-Norm and the Maximum-Norm with a certain degree of compensation. For future climate resilience decisions, it is important to consider all compensation methods in order to find the best solution for different problems.
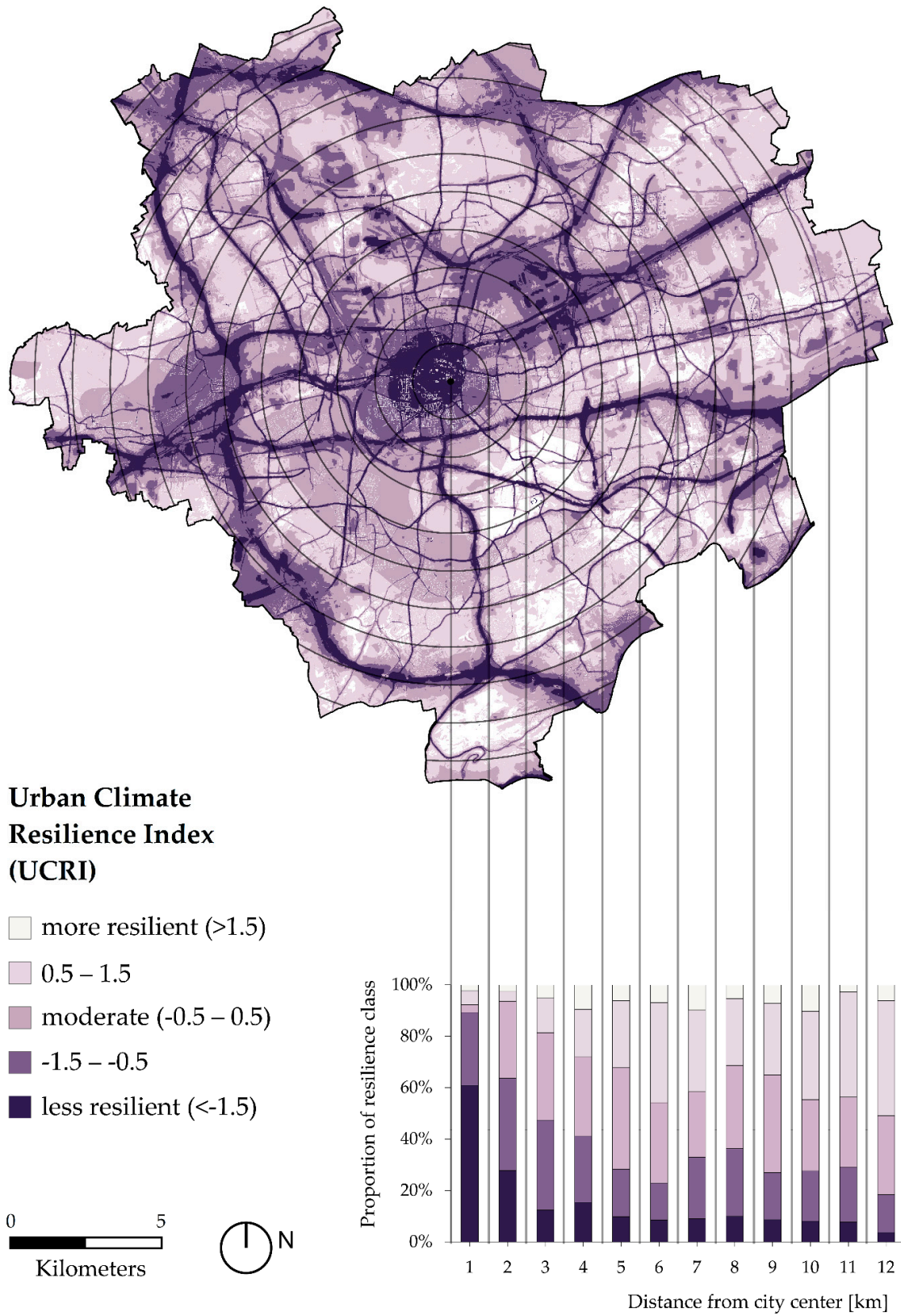
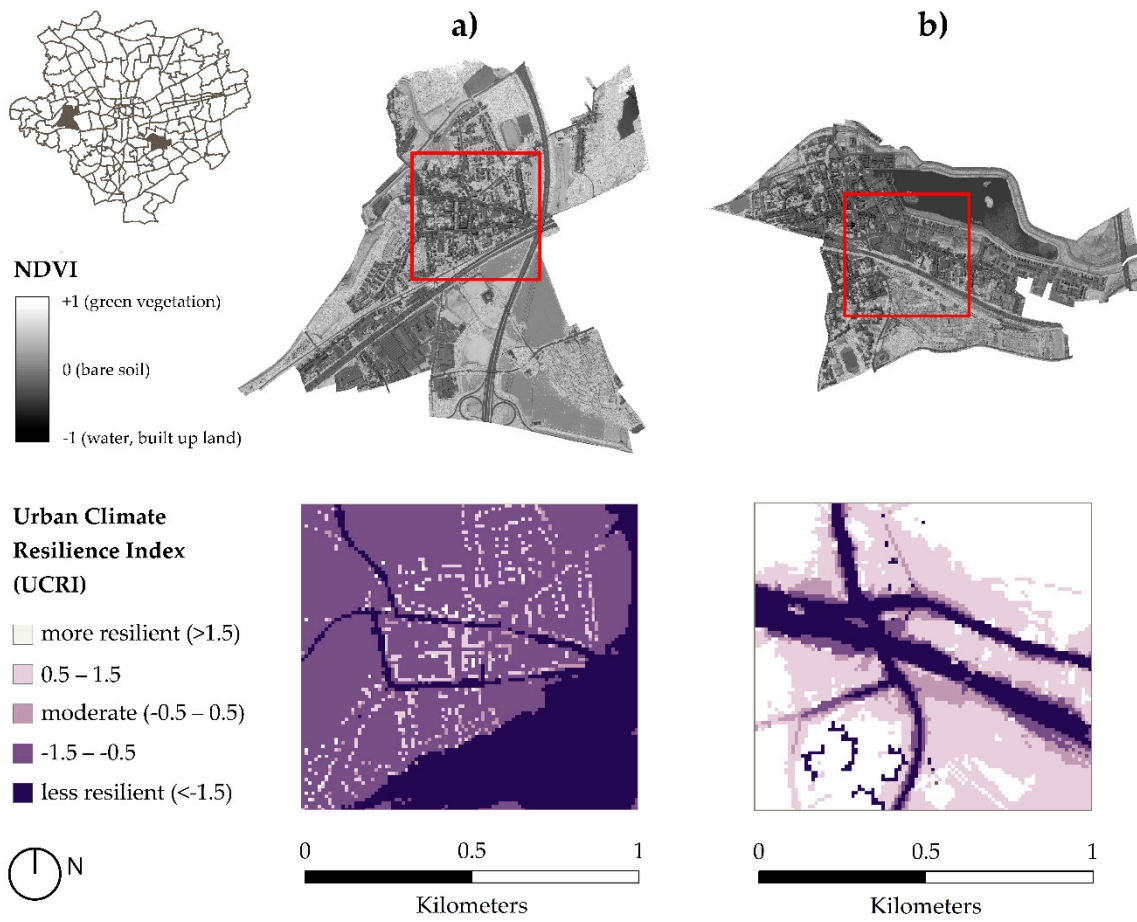**Figure 4.** Urban Climate Resilience Index (UCRI) in Dortmund.

Figure 5. Contrasts in Dortmund. Residential uses in (**a**) Marten sub-district, (**b**) Hörde and Clarenberg sub-districts.
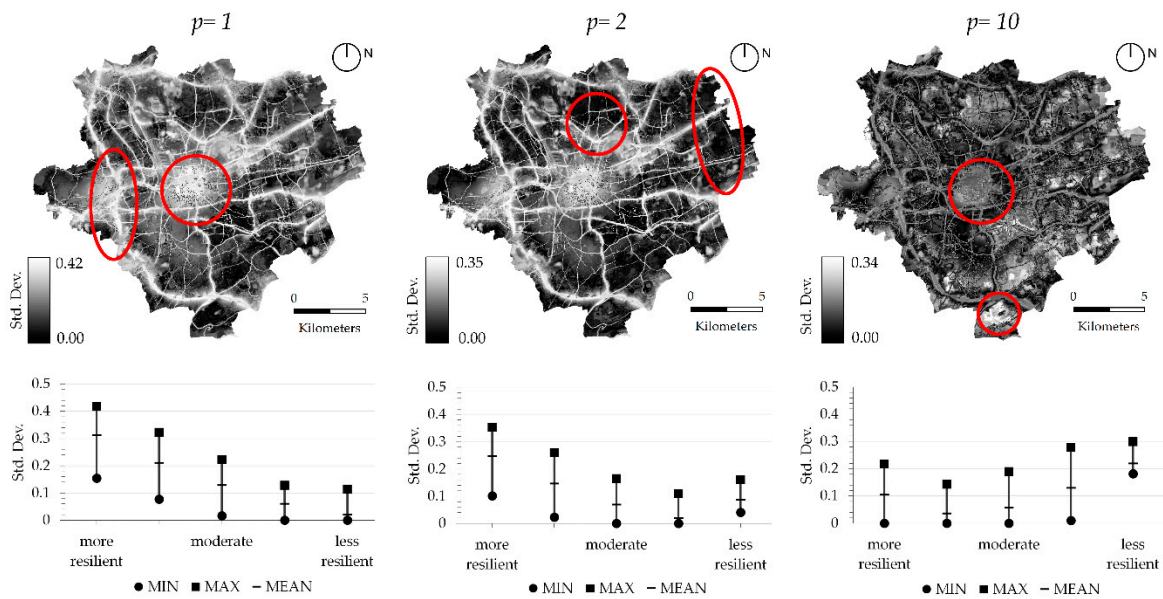

Figure 6. Standard deviation between Compromise Programming (CP) results and fuzzy logic regarding different compensation scenarios ($p = 1$, City-Block-Norm; $p = 2$, Euclidean-Norm; $p = 10$, Maximum-Norm).

6. Discussion and Conclusions

With this work we presented a GIS-based fuzzy logic analysis on climate resilience in the City of Dortmund. It was the aim of the authors to get an impression of how climate resilience can be quantified by indicators in a multidimensional manner and mapped both on municipality scale as well as on the neighborhood level. As quantitative proxies are a fundamental part of the process of resilience-building, our results allow a comparative overview of the spatial distribution of the robustness and adaptiveness for different subsystem dimensions with regard to social-ecological disparities. Nevertheless, the real reasons why certain disparities do exist, remain unknown.

Due to the fine resolution, the results can be implemented in future local climate adaptation plans or serve as an initiator for local grass roots projects concerning climate resilience and social-ecological disparities. Organized by the environmental planning office, on 5 December 2019 a participatory event for the integrated climate adaptation masterplan Dortmund (MiKaDo) was undergone with citizens, stakeholders and association members [112]. Initial ideas were collected and discussed with 68 participants, using parts of the resulted environmental maps in this paper for new climate adaptation strategies regarding green and open spaces, health related measurements as well as urban redevelopments (Figure 7). With this in mind, the results will be further discussed with the environmental planning office in the future.
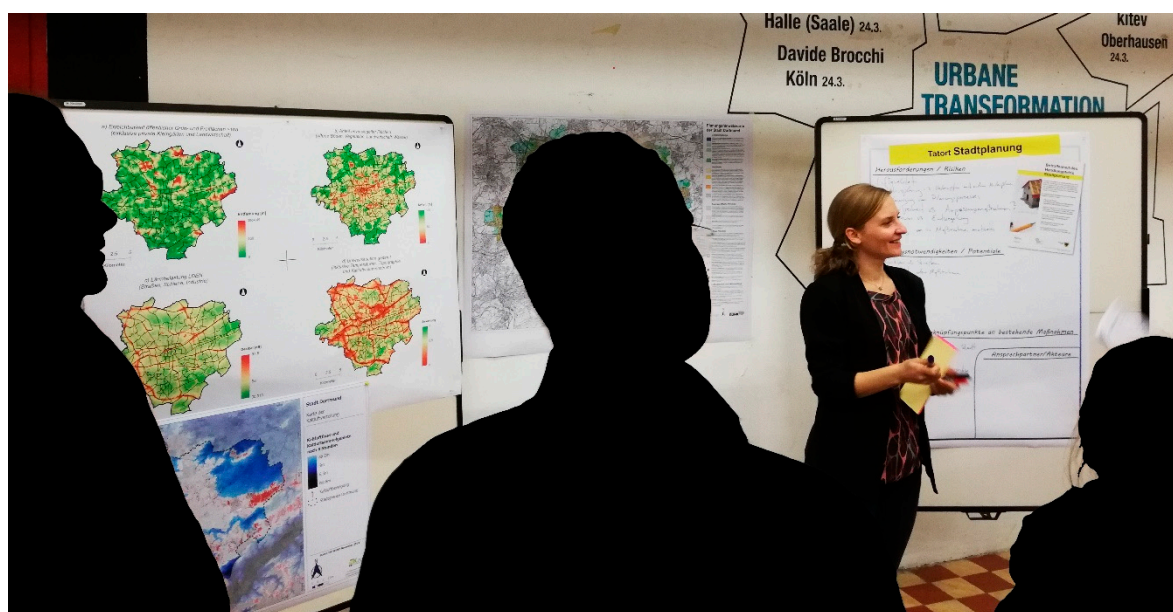

Figure 7. Impressions of the interactive discussion phase at the kick-off event for MiKaDo (source: authors' own).

Despite of the fact that the revealed results are new to the scale around resilience measurements, the method used is rather static and reactive, while resilience also embraces a dynamic picture. In order to accomplish this limitation, a second analysis and validation process with the same indicators should be carried out in the future to unveil new emerging or decreasing disparities and identify the relative importance of climatic against societal changes for future climate risks. From a methodological point of view, it would be interesting to change the arrangement of indicators and criteria in order to find out any differences in the output maps, whereas the development of individual rules in fuzzy logic modelling is a time-consuming issue. Some burdens like noise pollution or heat stress are directly noticeable, while air pollution may not be recognized when it is not related to smoke or odors. Therefore, it is also important to capture the perception of environmental threads by the individuals, whose results may completely differ from the presented approach.

Compared to previous studies on the accessibility of green and open spaces, the conducted network analysis revealed more realistic results [67]. However, this procedure is much more time-consuming and the results do not vary significantly from Euclidean distances, which is in line with the findings of Richter et al. [113]. Remote sensing plays an important role in monitoring resilience, as it provides a self-perpetuating, up-to-date, and often freely available digital geodatabase [114]. With this in mind, threatened areas can be examined without being physically on site, which enables the generation of pre- and post-disaster situation maps or evolutionary assessments of urban resilience in regular intervals [115]. Using the NDVI on a high spatial resolution was a noticeable benefit for the analysis, as it is also possible to capture the recovery of potential forest fires or urban flooding. Since heavy rainfalls are sudden onset events and heat waves are slow-onset ones, the temporal dimension should be considered, too. On the practical side, adequate spatial planning strategies and innovative on site measurements are needed. The population dasymetric mapping results delivered estimations close to reality. However, it is important to note that the results only represent synthetic allocations based on density values and land uses. The SHDI revealed satisfying results for the economic dimension. On the other hand, distributional effects of the economic sector should be brought into a regional context as well, especially in agglomerations like the Ruhr-Area. In this sense, our local small-scale approach may emerge unknown connections between regional large-scale disparities.

In the field of open geodata, especially in NRW the last two years have shown a huge step towards new possibilities in geoprocessing and small scale analysis, which in parallel encourages a certain transferability of the proposed method to other cities in this federal state in Germany. With this in mind, our indicator set can be scaled up to the regional level, which could be also interesting for regional planning authorities. However, some indicators are only possible to capture through local surveys, so there is still a need for municipalities to discuss the topic qualitatively with citizens. When it comes to resilience metrics, other indicators like economic loss or post-emergency costs could be worth to be included, but are also difficult to measure as these phenomena are indirect damages. In addition, populations change location over time, so that social dynamics should be taken into account in future monitoring purposes. This is also why population dynamics may be another indicator for the institutional subsystem, but it remains a geostatistical challenge to measure such processes on a fine scale. The same belongs to the availability of cars in case of an extreme event for evacuation capacity. Complementary, poverty is changing over time, too, as individuals can get into it, but also can get out of it. Individuals who are located in flood prone areas may choose their residence accepting the hazard and potential costs because of other factors, e.g., accessibility to working places. On the other hand, individuals who are unemployed may be "rich in relationships" and thus more able to cope with external crisis than better-off individuals [9]. Furthermore, climate plans and measurements do not always include local grass root activities within neighborhoods, which are also relevant to adaptation and mitigation "but not labelled as such" [105]. Health status, social skills (learning, transforming, etc.) or language abilities are also important factors for resilience preparedness assessment and may be included for sensitive groups in the future.

Although the presented method inherits some limitations regarding the institutional and economical resilience assessment, it provides a cost-effective workflow on assessing and visualizing climate resilience to identify potential weaknesses. Nonetheless, the full potential of measured phenomena by indicators only unfolds by investigating how they develop over time. Despite possible monitoring processes that could be carried out in the future, it is the real policy which shapes climate resilience. In this context, it is also to be observed whether future climate adaptation strategies exclude certain social and ethnic groups or even enhance existing disparities. There should be more research efforts on social-ecological systems feedbacks on climate extreme events across multiple spatial scales in order to assess the effectiveness, but also potential side effects of different policy fields.

Author Contributions: M.S. developed the methodology design, acquired necessary (geo-)data, performed the analysis, visualized the results and wrote the paper. N.X.T. substantially contributed to the conceptualization of the presented work and commented on the manuscript. S.G. reviewed and edited the manuscript and is the

coordinator of the research project Zukunft-Stadt-Region-Ruhr (ZUKUR). All authors have read and agreed to the published version of the manuscript.

Conflicts of Interest: The authors declare no conflict of interest.

Appendix A

Table A1. OSM-road types and corresponding max speed values used for network analyses.

Road Type	Max Speed
Motorway	120 km/h
Motorway_link	50 km/h
Trunk	120 km/h
Trunk_link	50 km/h
Primary	50 km/h
Primary_link	40 km/h
Secondary	50 km/h
Secondary_link	40 km/h
Tertiary	50 km/h
Tertiary_link	40 km/h
Residential	30 km/h
Living_street	5 km/h
Service	20 km/h
Track	20 km/h
Unclassified	30 km/h

Table A2. Critical and sensitive infrastructures used including ALKIS-Codes.

| Sectors	Subsectors	ALKIS-Code
Energy	Electricity, Gas, Oil	2571, 2580, 2590, 2520, 2523, 2501, 2570, 2130, 2522
Information technology and telecommunications	Telecommunications, Information Technology	3035, 2540
Transport and traffic	Air transport, Inland waterways transport, Rail transport, Road transport	42,015, 42,016, 42,010, 42,001
Health	Medical services, Pharmaceuticals and vaccines, Laboratories, hospitals, old people's homes, shelter for homeless	1022, 3050, 3051, 3052, 2056, 3053, 3064
Water	Public water supply, Public sewage disposal	2610, 2611, 2510, 2512, 2513
Finance and insurance industry	Banks, Stock exchanges, Insurance companies, Financial service providers	2020, 2030, 2040
Government and public administration	Government and public administration, Judicial bodies, Emergency/rescue services including civil protection	3066, 3010, 3011, 3012, 3014, 3015, 3016, 3019, 3071, 3072, 3070, 3100
Media and culture	Broadcasting (television and radio), print and electronic media, Cultural property, Structures of symbolic meaning	2171, 3030, 3060, 3040, 3041, 3033, 3032, 3034, 3031, 3036

Appendix B
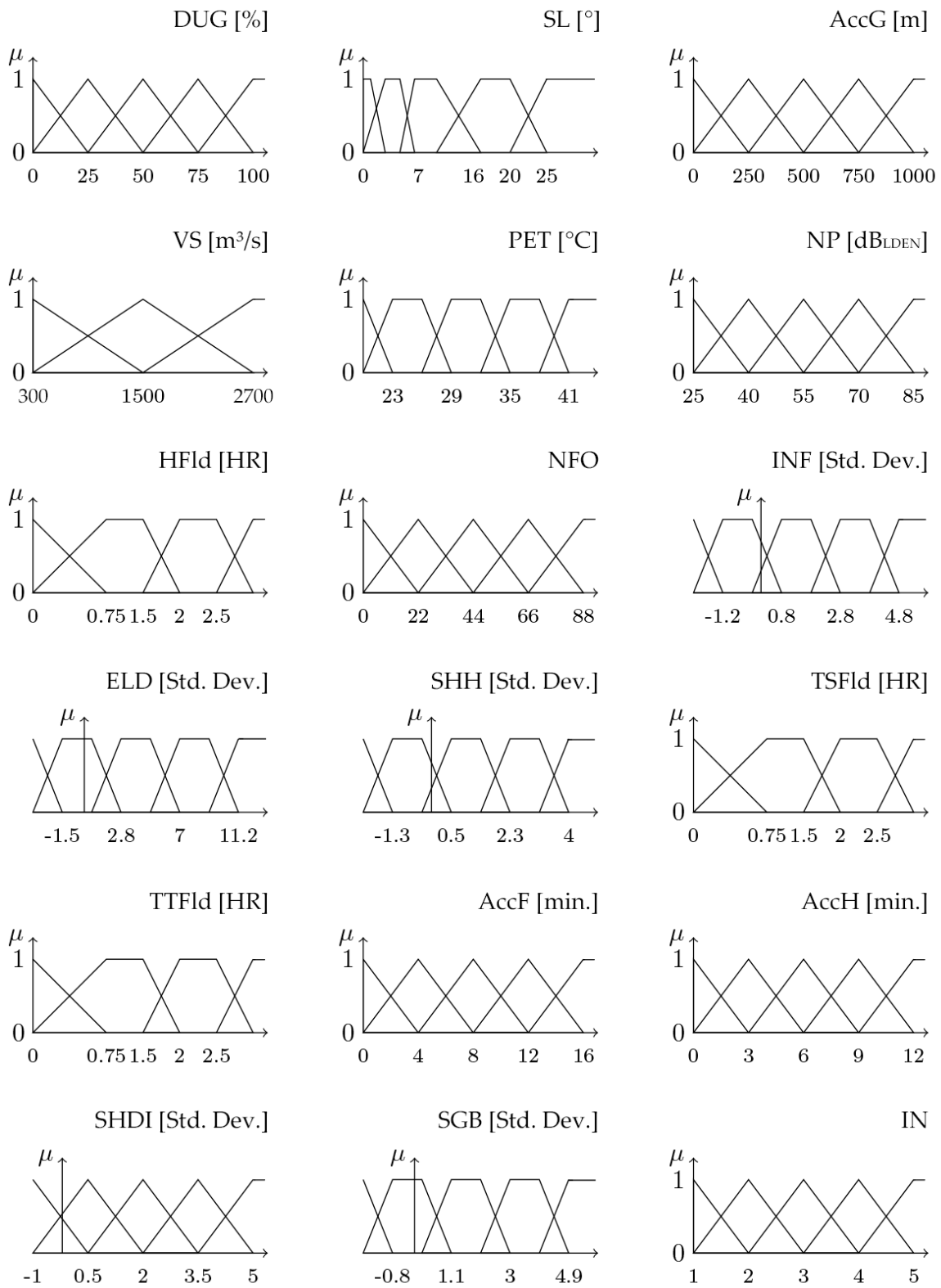
Figure A1. Fuzzy membership functions for the selected indicators.

References

1. Hagedorn, G.; Kalmus, P.; Mann, M.; Vicca, S.; van den Berge, J.; van Ypersele, J.-P.; Bourg, D.; Rotmans, J.; Kaaronen, R.; Rahmstorf, S.; et al. Concerns of young protesters are justified. *Science* **2019**, 139–140. [CrossRef]
2. Allgaier, J. Science and Environmental Communication on YouTube: Strategically Distorted Communications in Online Videos on Climate Change and Climate Engineering. *Front. Commun.* **2019**, *4*, 36. [CrossRef]
3. United Nations, Economic and Social Affairs. World Urbanization Prospects: The 2018 Revision. 2018. Available online: https://population.un.org/wup/Publications/Files/WUP2018-KeyFacts.pdf (accessed on 4 July 2019).
4. European Environment Agency (EEA). Economic Losses from Climate-Related Extremes in Europe. 2019. Available online: https://www.eea.europa.eu/data-and-maps/indicators/direct-losses-from-weather-disasters-3/assessment-2 (accessed on 1 July 2019).
5. Imbery, F.; Friedrich, K.; Haeseler, S.; Koppe, C.; Janssen, W.; Bissolli, P. Vorläufiger Rückblick auf den Sommer 2018—Eine Bilanz Extremer Wetterereignisse. Available online: https://www.dwd.de/DE/leistungen/besondereereignisse/temperatur/20180803_bericht_sommer2018.pdf?__blob=publicationFile&v=10 (accessed on 29 October 2018).
6. Imbery, F.; Friedrich, K.; Koppe, C.; Janssen, W.; Pfeifroth, U.; Daßler, J.; Bissolli, P. 2018 Wärmster Sommer im Norden und Osten Deutschlands. Stand 6 September 2018. Available online: https://www.dwd.de/DE/leistungen/besondereereignisse/temperatur/20180906_waermstersommer_nordenosten2018.pdf?__blob=publicationFile&v=7 (accessed on 13 November 2018).
7. Walker, B.H.; Salt, D.A. *Resilience Thinking: Sustaining Ecosystems and People in a Changing World*; Island Press: Washington, DC, USA, 2006; ISBN 9781597260930.
8. Caniglia, B.S.; Frank, B.; Delano, D.; Kerner, B. Enhancing environmental justice research and praxis: The inclusion of human security, resilience and vulnerabilities literature. *IJISD* **2014**, *8*, 409. [CrossRef]
9. Friend, R.; Moench, M. What is the purpose of urban climate resilience? Implications for addressing poverty and vulnerability. *Urban Clim.* **2013**, *6*, 98–113. [CrossRef]
10. Sandoval, V.; Gonzalez-Muzzio, C.; Albornoz, C. Resilience and Environmental Justice: Potential Linkages. *Procedia Econ. Financ.* **2014**, *18*, 416–424. [CrossRef]
11. Pellow, D.N. Environmental Inequality Formation: Toward a Theory of Environmental Injustice. *Am. Behav. Sci.* **2000**, *43*, 581–601. [CrossRef]
12. Mayer, B. A framework for improving resilience. In *Resilience, Environmental Justice and the City*; Caniglia, B.S., Vallée, M., Frank, B.F., Eds.; Routledge: Abingdon/Oxon, UK; New York, NY, USA, 2017; pp. 37–56. ISBN 9781138119895.
13. Collier, M.J.; Nedović-Budić, Z.; Aerts, J.; Connop, S.; Foley, D.; Foley, K.; Newport, D.; McQuaid, S.; Slaev, A.; Verburg, P. Transitioning to resilience and sustainability in urban communities. *Cities* **2013**, *32*, S21–S28. [CrossRef]
14. Denton, F.; Wilbanks, T.J.; Abeysinghe, A.C.; Burton, I.; Gao, Q.; Lemos, M.C.; Masui, T.; O'Brien, K.L.; Warner, K. Climate-resilient pathways: Adaptation, mitigation, and sustainable development I. In *Climate Change 2014: Impacts, Adaptation, and Vulnerability. Part A: Global and Sectoral Aspects. Contribution of Working Group II to the Fifth Assessment Report of the Intergovernmental Panel on Climate Change*; Field, C.B., Barros, V.R., Dokken, D.J., Mach, K.J., Mastrandrea, M.D., Bilir, T.E., Chatterjee, M., Ebi, K.L., Estrada, Y.O., Genova, R.C., Eds.; Cambridge University Press: Cambridge, UK; New York, NY, USA, 2014; pp. 1101–1131.
15. Davoudi, S. Just Resilience. *City Community* **2018**, *17*, 3–7. [CrossRef]
16. Greiving, S.; Arens, S.; Becker, D.; Fleischhauer, M.; Hurth, F. Improving the Assessment of Potential and Actual Impacts of Climate Change and Extreme Events Through a Parallel Modeling of Climatic and Societal Changes at Different Scales. *J. Extrem. Events* **2017**, *4*, 1850003. [CrossRef]
17. Folke, C. Resilience (Republished). *ES* **2016**, *21*. [CrossRef]
18. Meerow, S.; Stults, M. Comparing Conceptualizations of Urban Climate Resilience in Theory and Practice. *Sustainability* **2016**, *8*, 701. [CrossRef]
19. Christmann, G.; Balgar, K.; Mahlkow, N. Local Constructions of Vulnerability and Resilience in the Context of Climate Change. A Comparison of Lübeck and Rostock. *Soc. Sci.* **2014**, *3*, 142–159. [CrossRef]
20. Cutter, S.L.; Burton, C.G.; Emrich, C.T. Disaster Resilience Indicators for Benchmarking Baseline Conditions. *J. Homel. Secur. Emerg. Manag.* **2010**, 7. [CrossRef]

21. Davoudi, S.; Shaw, K.; Haider, L.J.; Quinlan, A.E.; Peterson, G.D.; Wilkinson, C.; Fünfgeld, H.; McEvoy, D.; Porter, L. Resilience: A Bridging Concept or a Dead End? *Plan. Theory Pract.* **2012**, *13*, 299–333. [CrossRef]

22. Zadeh, L.A. Fuzzy sets. *Inf. Control* **1965**, *8*, 338–353. [CrossRef]

23. Bundesministerium für Bildung und Forschung (BMBF). Zukunftsstadt. Strategische Forschungs-Und Innovationsagenda. 2015. Available online: https://www.fona.de/mediathek/pdf/Zukunftsstadt.pdf (accessed on 12 May 2019).

24. Werner, E.E.; Bierman, J.M.; French, F.E. *The Children of Kauai. A longitudinal Study from the Prenatal Period to Age Ten*; University of Hawaii Press: Honolulu, HI, USA, 1971; ISBN 0870228609.

25. Holling, C.S. Resilience and Stability of Ecological Systems. *Annu. Rev. Ecol. Syst.* **1973**, *4*, 1–23. [CrossRef]

26. Adewale, S.; Godson, A.; Sokan-Adeaga, A.; Sokan-Adeaga, M.; Deborah, E. Resilience and Sustainability of the Ecosystem: An Environmental Health Perspective. *Lond. J. Res. Sci. Nat. Form.* **2018**, *18*, 7–26.

27. Mileti, D.; Noji, E.K. *Disasters by Design: A Reassessment of Natural Hazards in the United States*; Joseph Henry Press: Washington, DC, USA, 1999; ISBN 978-0-309-26173-9.

28. European Commission, Directorate-General for Environment. *Guidance on Integrating Climate Change and Biodiversity into Strategic Environmental Assessment*; Publications Office: Luxembourg, 2013; ISBN 978-92-79-29016-9.

29. Fekkak, M.; Fleischhauer, M.; Greiving, S.; Lucas, R.; Schinkel, J.; von Winterfeld, U. "Resiliente Stadt-Zukunftsstadt". Im Auftrag des Ministeriums für Bauen, Wohnen, Stadtentwicklung und Verkehr des Landes Nordrhein-Westfalen (MBWSV); Forschungsgutachten November 2016. Available online: https://epub.wupperinst.org/frontdoor/deliver/index/docId/6614/file/6614_Resiliente_Stadt.pdf (accessed on 14 January 2020).

30. Wilbanks, T.J. Integrating climate change and sustainable development in a place-based context. *Clim. Policy* **2003**, *3*, 147–154. [CrossRef]

31. World Commission on Environment and Development (WCED). *Our Common Future: Towards Sustainable Development*; WCED: Oxford, UK, 1987.

32. Birkmann, J.; Bach, C.; Vollmer, M. Tools for Resilience Building and Adaptive Spatial Governance. *Raumforsch. Raumordn.* **2012**, *70*, 293–308. [CrossRef]

33. Hassler, U.; Kohler, N. Resilience in the built environment. *Build. Res. Inf.* **2014**, *42*, 119–129. [CrossRef]

34. Wang, Y.; Du, M.; Zhou, L.; Cai, G.; Bai, Y. A Novel Evaluation Approach of County-Level City Disaster Resilience and Urban Environmental Cleanliness Based on SDG11 and Deqing County's Situation. *Sustainability* **2019**, *11*, 5713. [CrossRef]

35. Meerow, S.; Newell, J.P.; Stults, M. Defining urban resilience: A review. *Landsc. Urban Plan.* **2016**, *147*, 38–49. [CrossRef]

36. Moser, S.; Meerow, S.; Arnott, J.; Jack-Scott, E. The turbulent world of resilience: Interpretations and themes for transdisciplinary dialogue. *Clim. Chang.* **2019**, *153*, 21–40. [CrossRef]

37. Cutter, S.L. The landscape of disaster resilience indicators in the USA. *Nat. Hazards* **2016**, *80*, 741–758. [CrossRef]

38. Wu, J.; Wu, T. Ecological Resilience as a Foundation for Urban Design and Sustainability. In *Resilience in Ecology and Urban Design*; Pickett, S.T.A., Cadenasso, M.L., McGrath, B., Eds.; Springer: Dordrecht, The Netherlands, 2013; pp. 211–229. ISBN 978-94-007-5340-2.

39. Figueiredo, L.; Honiden, T.; Schumann, A. *Indicators for Resilient Cities*; OECD Regional Development Working Papers; OECD Publishing: Paris, France, 2018.

40. Feldmeyer, D.; Wilden, D.; Kind, C.; Kaiser, T.; Goldschmidt, R.; Diller, C.; Birkmann, J. Indicators for Monitoring Urban Climate Change Resilience and Adaptation. *Sustainability* **2019**, *11*, 2931. [CrossRef]

41. Abramson, D.M.; Grattan, L.M.; Mayer, B.; Colten, C.E.; Arosemena, F.A.; Bedimo-Rung, A.; Lichtveld, M. The resilience activation framework: A conceptual model of how access to social resources promotes adaptation and rapid recovery in post-disaster settings. *J. Behav. Health Serv. Res.* **2015**, *42*, 42–57. [CrossRef]

42. Neil Adger, W.; Arnell, N.W.; Tompkins, E.L. Successful adaptation to climate change across scales. *Glob. Environ. Chang.* **2005**, *15*, 77–86. [CrossRef]

43. Xu, L.; Marinova, D.; Guo, X. Resilience thinking: A renewed system approach for sustainability science. *Sustain. Sci.* **2015**, *10*, 123–138. [CrossRef]

44. Leichenko, R. Climate change and urban resilience. *Curr. Opin. Environ. Sustain.* **2011**, *3*, 164–168. [CrossRef]

45. Platt, S.; Brown, D.; Hughes, M. Measuring resilience and recovery. *Int. J. Disaster Risk Reduct.* **2016**, *19*, 447–460. [CrossRef]

46. Weichselgartner, J.; Kelman, I. Geographies of resilience. *Prog. Hum. Geogr.* **2015**, *39*, 249–267. [CrossRef]

47. Nelson, D.R.; Adger, W.N.; Brown, K. Adaptation to Environmental Change: Contributions of a Resilience Framework. *Annu. Rev. Environ. Resour.* **2007**, *32*, 395–419. [CrossRef]

48. Adger, W.N. Social and ecological resilience: Are they related? *Prog. Hum. Geogr.* **2000**, *24*, 347–364. [CrossRef]

49. Willows, R. (Ed.) *Climate Adaptation. Risk, Uncertainty and Decision-Making*; UK Climate Impacts Programme: Oxford, UK, 2003; ISBN 9780954483005.

50. Kötter, T.; Weiß, D. *Stresstest Stadt—Wie Resilient Sind Unsere Städte? Unsicherheiten der Stadtentwicklung Identifizieren, Analysieren und Bewerten; Stand: February 2018*; Bundesinstitut für Bau-, Stadt und Raumforschung (BBSR) im Bundesamt für Bauwesen und Raumordnung (BBR): Bonn, Germany, 2018; ISBN 978-3-87994-224-4.

51. Folke, C.; Carpenter, S.; Walker, B.; Scheffer, M.; Chapin, T.; Rockström, J. Resilience thinking: Integrating resilience, adaptability and transformability. *Ecol. Soc.* **2010**, *15*, 1–9. [CrossRef]

52. Choko, O.P.; Schmitt Olabisi, L.; Onyeneke, R.U.; Chiemela, S.N.; Liverpool-Tasie, L.S.O.; Rivers, L. A Resilience Approach to Community-Scale Climate Adaptation. *Sustainability* **2019**, *11*, 3100. [CrossRef]

53. Renschler, C.S.; Frazier, A.E.; Arendt, L.A.; Cimellaro, G.P.; Reinhorn, A.M.; Bruneau, M. *A Framework for Defining and Measuring Resilience at the Community Scale: The PEOPLES Resilience Framework*; University of Buffalo State University of New York: Buffalo, NY, USA, 2010.

54. The Nature Conservancy. TNC Coastal Resilience Tool. Available online: http://coastalresilience.org/natural-solutions/toolkit/ (accessed on 26 October 2018).

55. Winderl, T. Disaster Resilience Measurements: Stocktaking of Ongoing Efforts in Developing Systems for Measuring Resilience. Available online: https://www.preventionweb.net/files/37916_disasterresiliencemeasurementsundpt.pdf (accessed on 26 October 2018).

56. Rockefeller Foundation. 100 Resilient Cities. Available online: http://www.100resilientcities.org/ (accessed on 21 June 2019).

57. Resilience Alliance. Available online: https://www.resalliance.org/ (accessed on 21 June 2019).

58. Pestel Institut. Regionale Krisenfestigkeit: Eine Indikatorengestützte Bestandsaufnahme auf der Ebene der Kreise und Kreisfreien Städte. Available online: https://www.braunschweig.de/politik_verwaltung/fb_institutionen/staedtische_gesellschaften/bsmportal/spitzenposition/Regionale-Krisenfestigkeit-Pestel-Institut_011211.pdf (accessed on 5 June 2019).

59. Brunetta, G.; Salata, S. Mapping Urban Resilience for Spatial Planning—A First Attempt to Measure the Vulnerability of the System. *Sustainability* **2019**, *11*, 2331. [CrossRef]

60. Moghadas, M.; Asadzadeh, A.; Vafeidis, A.; Fekete, A.; Kötter, T. A multi-criteria approach for assessing urban flood resilience in Tehran, Iran. *Int. J. Disaster Risk Reduct.* **2019**, *35*, 101069. [CrossRef]

61. Jelinski, D.E.; Wu, J. The modifiable areal unit problem and implications for landscape ecology. *Landsc. Ecol* **1996**, *11*, 129–140. [CrossRef]

62. Stadt Dortmund, Stabsstelle Dortmunder Statistik. *Jahresber. Bevölk.* **2019**, *206*, 1–48.

63. Stadt Dortmund. 20. Jahrhundert—"Heute": Strukturkrise und-Wandel. Available online: https://www.dortmund.de/de/leben_in_dortmund/ausunsererstadt/stadtportraet/stadtgeschichte/20jahrhundert/strukturkrise_und_wandel/index.html (accessed on 9 September 2019).

64. Strohmeier, K.P.; Bader, S. Demographic Decline, Segregation, and Social Urban Renewal in Old Industrial Metropolitan Areas. Available online: https://difu.de/publikationen/demographic-decline-segregation-and-social-urban-renewal-in.html (accessed on 9 September 2019).

65. Greiving, S.; Pratzler-Wanczura, S.; Sapountzaki, K.; Ferri, F.; Grifoni, P.; Firus, K.; Xanthopoulos, G. Linking the actors and policies throughout the disaster management cycle by "Agreement on Objectives"—A new output-oriented management approach. *Nat. Hazards Earth Syst. Sci.* **2012**, *12*, 1085–1107. [CrossRef]

66. Greiving, S.; Lindner, C. Assessment of Flash Flood Risk in a Continuous Urban Fabric by the Example of the City of Dortmund. In *Urban Flood Risk Management—Approaches to Enhance Resilience of Communities*; Zenz, G., Hornich, R., Eds.; Verlag der Technischen Universität Graz: Graz, Austria, 2011; pp. 257–262.

67. Shrestha, R.; Flacke, J.; Martinez, J.; van Maarseveen, M. Environmental Health Related Socio-Spatial Inequalities: Identifying "Hotspots" of Environmental Burdens and Social Vulnerability. *Int. J. Environ. Res. Public Health* **2016**, *13*, 691. [CrossRef] [PubMed]

68. Flacke, J.; Schüle, S.A.; Köckler, H.; Bolte, G. Mapping Environmental Inequalities Relevant for Health for Informing Urban Planning Interventions-A Case Study in the City of Dortmund, Germany. *Int. J. Environ. Res. Public Health* **2016**, *13*, 711. [CrossRef] [PubMed]

69. Caffier, A.; Elsner, C.; Rath, C.; Robens, F.; Seidel, J.; Will, K. Offene Geobasisdaten für NRW. *Z. Geodäsie Geoinf. Landmanag. (Zfv)* **2017**, *142*, 133–145.

70. McGarigal, K. FRAGSTATS HELP. Available online: http://www.umass.edu/landeco/research/fragstats/documents/fragstats.help.4.2.pdf (accessed on 14 September 2017).

71. McGarigal, K. FRAGSTATS: Spatial Pattern Analysis Program for Categorical Maps. Available online: https://www.umass.edu/landeco/research/fragstats/downloads/fragstats_downloads.html (accessed on 9 January 2020).

72. Wieland, R.; Voss, M.; Holtmann, X.; Mirschel, W.; Ajibefun, I. Spatial Analysis and Modeling Tool (SAMT): 1. Structure and possibilities. *Ecol. Inform.* **2006**, *1*, 67–76. [CrossRef]

73. Leibniz-Zentrum für Agrarlandschaftsforschung (ZALF) e. V. Müncheberg. Programme zum Herunterladen—ZALF. Available online: http://www.zalf.de/de/forschung_lehre/software_downloads/Seiten/default.aspx (accessed on 9 January 2020).

74. Comber, A.; Brunsdon, C.; Green, E. Using a GIS-based network analysis to determine urban greenspace accessibility for different ethnic and religious groups. *Landsc. Urban Plan.* **2008**, *86*, 103–114. [CrossRef]

75. Schwarze, B. Eine Methode zum Messen von Naherreichbarkeit in Kommunen. Ph.D. Thesis, TU Dortmund University, Dortmund, Germany, 14 July 2015.

76. Brugge, D.; Patton, A.P.; Bob, A.; Reisner, E.; Lowe, L.; Bright, O.-J.M.; Durant, J.L.; Newman, J.; Zamore, W. Developing Community-Level Policy and Practice to Reduce Traffic-Related Air Pollution Exposure. *Environ. Justice* **2015**, *8*, 95–104. [CrossRef]

77. Gilmore, S.; Saleem, A.; Dewan, A. Effectiveness of DOS (Dark-Object Subtraction) method and water index techniques to map wetlands in a rapidly urbanising megacity with Landsat 8 data. In Proceedings of the Research@Locate in Conjunction with the Annual Conference on Spatial Information in Australia and New Zealand, Brisbane, Australia, 10–12 March 2015; pp. 100–108.

78. Zadeh, L.A. Toward a theory of fuzzy information granulation and its centrality in human reasoning and fuzzy logic. *Fuzzy Sets Syst.* **1997**, *90*, 111–127. [CrossRef]

79. Zhang, Z.; Sheng, L.; Yang, J.; Chen, X.-A.; Kong, L.; Wagan, B. Effects of Land Use and Slope Gradient on Soil Erosion in a Red Soil Hilly Watershed of Southern China. *Sustainability* **2015**, *7*, 14309–14325. [CrossRef]

80. Honold, J.; Beyer, R.; Lakes, T.; van der Meer, E. Multiple environmental burdens and neighborhood-related health of city residents. *J. Environ. Psychol.* **2012**, *32*, 305–317. [CrossRef]

81. Zheng, Y.; Xie, X.-L.; Lin, C.-Z.; Wang, M.; He, X.-J. Development as adaptation: Framing and measuring urban resilience in Beijing. *Adv. Clim. Chang. Res.* **2018**, *9*, 234–242. [CrossRef]

82. Krüger, T.; Held, F.; Hoechstetter, S.; Goldberg, V.; Geyer, T.; Kurbjuhn, C. A new heat sensitivity index for settlement areas. *Urban Clim.* **2013**, *6*, 63–81. [CrossRef]

83. Bach, C.; Birkmann, J.; Kropp, J.; Olonscheck, M.; Setiadi, N.; Vollmer, M.; Walther, C. *Assessing Vulnerability to Heat Waves and Heavy Rainfall at a Community Level*, 11st ed.; Federal Office of Civil Protection and Disaster Assistence (BBK): Bonn, Germany, 2014; pp. 1–157.

84. Bradford, K.; Abrahams, L.; Hegglin, M.; Klima, K. A Heat Vulnerability Index and Adaptation Solutions for Pittsburgh, Pennsylvania. *Environ. Sci. Technol.* **2015**, *49*, 11303–11311. [CrossRef] [PubMed]

85. Kiran, K.C.; Corcoran, J.; Chhetri, P. Measuring the spatial accessibility to fire stations using enhanced floating catchment method. *Socio-Econ. Plan. Sci.* **2018**, 100673. [CrossRef]

86. Caniglia, B.S.; Frank, B. Revealing the resilience infrastructure of cities: Preventing environmental injustices-in-waiting. In *Resilience, Environmental Justice and the City*; Caniglia, B.S., Vallée, M., Frank, B.F., Eds.; Routledge: Abingdon/Oxon, UK; New York, NY, USA, 2017; pp. 57–75. ISBN 9781138119895.

87. Palka, G.; Grădinaru, S.R.; Jørgensen, G.; Hersperger, A.M. Visualizing Planning Intentions: From Heterogeneous Information to Maps. *J. Geovisualizat. Spat. Anal.* **2018**, *2*, 617. [CrossRef]

88. Telesca, L.; Lasaponara, R. Pre- and post-fire behavioral trends revealed in satellite NDVI time series. *Geophys. Res. Lett.* **2006**, *33*, 2293. [CrossRef]

89. Halkia, M.; Ferri, S.; Siragusa, A.; Pafi, M. *Measuring the Accessibility of Urban Green Areas. A Comparison of the Green ESM with Other Datasets in Four European Cities*; Publications Office: Luxembourg, 2016; ISBN 9279612867.

90. Schaefer, M.; Thinh, N.X. Evaluation of Land Cover Change and Agricultural Protection Sites: A GIS and Remote Sensing Approach for Ho Chi Minh City, Vietnam. *Heliyon* **2019**, *5*, e01773. [CrossRef]

91. Sobrino, J.A.; Jiménez-Muñoz, J.C.; Paolini, L. Land surface temperature retrieval from LANDSAT TM 5. *Remote Sens. Environ.* **2004**, *90*, 434–440. [CrossRef]

92. Wang, F.; Qin, Z.; Song, C.; Tu, L.; Karnieli, A.; Zhao, S. An Improved Mono-Window Algorithm for Land Surface Temperature Retrieval from Landsat 8 Thermal Infrared Sensor Data. *Remote Sens.* **2015**, *7*, 4268–4289. [CrossRef]

93. Avdan, U.; Jovanovska, G. Algorithm for Automated Mapping of Land Surface Temperature Using LANDSAT 8 Satellite Data. *J. Sens.* **2016**, *2016*, 1480307. [CrossRef]

94. Matzarakis, A.; Amelung, B. Physiological Equivalent Temperature as Indicator for Impacts of Climate Change on Thermal Comfort of Humans. In *Seasonal Forecasts, Climatic Change and Human Health*; Thomson, M.C., Garcia-Herrera, R., Beniston, M., Eds.; Springer: Dordrecht, The Netherlands, 2008; pp. 161–172. ISBN 978-1-4020-6876-8.

95. European Environment Agency. *Noise in Europe 2014*; Publications Office: Luxembourg, 2014; ISBN 9292135058.

96. Directive 2002/49/EC of the European Parliament and of the Council Relating to the Assessment and Management of Environmental Noise. 2002. Available online: https://eur-lex.europa.eu/LexUriServ/LexUriServ.do?uri=OJ:L:2002:189:0012:0025:EN:PDF (accessed on 14 January 2020).

97. Foudi, S.; Osés-Eraso, N.; Tamayo, I. Integrated spatial flood risk assessment: The case of Zaragoza. *Land Use Policy* **2015**, *42*, 278–292. [CrossRef]

98. DEFRA. *R&D Outputs: Flood Risks to People Phase 2. FD2321/TR2 Guidance Document*; DEFRA: London, UK, 2006.

99. Taubenböck, H.; Wurm, M.; Klein, I.; Esch, T. Verwundbarkeitsanalyse urbaner Räume: Ableitung von Indikatoren aus multisensoralen Fernerkundungsdaten. In *REAL CORP 2011: Change for Stability: Lifecycles of Cities and Regions: The Role and Possibilities of Foresighted Planning in Transformation Process, Proceedings of the 16th International Conference on Urban Planning, Regional Development and Information Society = Beiträge zur 16. Internationalen Konferenz zu Stadtplanung, Regionalentwicklung und Informationsgesellschaft, Essen, Germany, 18–20 May 2011*; Schrenk, M., Popovich, V., Zeile, P., Eds.; CORP, Competence Center of Urban and Regional Planning: Schwechat-Rannersdorf, Austria, 2011; pp. 1107–1118. ISBN 978-3-9503110-1-3.

100. Mileu, N.; Queirós, M. Development of a QGIS Plugin to Dasymetric Mapping. *Free Open Source Softw. Geospat. (Foss4g) Conf. Proc.* **2018**, *18*. [CrossRef]

101. Holloway, S.; Schumacher, J.; Redmond, R. *People & Place: Dasymetric Mapping Using Arc/Info*; High Mountain Press: Missoula, MT, USA, 1997.

102. Federal Ministry of the Interior (BMI). National Strategy for the Protection of Critical Infrastructures (KRITIS-Strategie). Available online: https://www.bmi.bund.de/SharedDocs/downloads/DE/publikationen/themen/bevoelkerungsschutz/kritis.html (accessed on 27 July 2019).

103. Stein, J. *Qualitätskriterien für die Bedarfsplanung von Feuerwehren in Städten*; AGBF-Bund: Bonn, Germany, 2015.

104. Gonçalves, C.; Marques da Costa, E. *Framework and Indicators to Measure Urban Resilience: Assay in Caldas da Rainha and Évora. Urban Systems*; AESOP/ACSP Congress: Dublin, Ireland, 2013.

105. Reckien, D.; Flacke, J.; Dawson, R.J.; Heidrich, O.; Olazabal, M.; Foley, A.; Hamann, J.J.-P.; Orru, H.; Salvia, M.; de Gregorio Hurtado, S.; et al. Climate change response in Europe: What's the reality? Analysis of adaptation and mitigation plans from 200 urban areas in 11 countries. *Clim. Chang.* **2014**, *122*, 331–340. [CrossRef]

106. Kayacan, E.; Khanesar, M.A. *Fundamentals of Type-1 Fuzzy Logic Theory. Fuzzy Neural Networks for Real Time Control Applications*; Elsevier: Amsterdam, The Netherlands, 2016; pp. 13–24. ISBN 9780128026878.

107. Piegat, A. *Fuzzy Modeling and Control*; Physica-Verlag HD: Heidelberg, Germany, 2001; ISBN 9783790824865.

108. Thinh, N.X.; Hedel, R. Vergleich zwei räumlicher Bewertungsmethoden-Compromise Programming und regelbasierte hierarchische Fuzzy-Bewertung. In *Simulation in Umwelt-und Geowissenschaften*; Wittmann, J., Thinh, N.X., Eds.; Umweltinformatik, Shaker Verlag: Aachen, Germany, 2005; pp. 57–66.

109. Saaty, T.L. Decision making with the analytic hierarchy process. *Int. J. Serv. Sci.* **2008**, *1*, 83–98. [CrossRef]

110. Haddad, B.M. Ranking the adaptive capacity of nations to climate change when socio-political goals are explicit. *Glob. Environ. Chang.* **2005**, *15*, 165–176. [CrossRef]

111. Zeleny, M. *Multiple Criteria Decision Making. Kyoto, 1975*; Springer: Berlin, Germany, 1976; ISBN 0387076840.

112. Lokalkompass Dortmund-Ost. Projektauftakt: Masterplan Integrierte Klimaanpassung Dortmund (MiKaDo). Available online: https://www.lokalkompass.de/dortmund/c-politik/projektauftakt-masterplan-integrierte-klimaanpassung-dortmund-mikado_a1260159 (accessed on 9 December 2019).

113. Richter, B.; Grunewald, K.; Meinel, G. Analyse von Wegedistanzen in Städten zur Verifizierung des Ökosystemleistungsindikators "Erreichbarkeit städtischer Grünflächen". In *AGIT 2-2016: Journal für Angewandte Geoinformatik, 1., Neuerscheinung*; Strobl, J., Zagel, B., Griesebner, G., Blaschke, T., Wichmann, H., Eds.; Wichmann Verlag: Berlin, Germany, 2016; pp. 472–481. ISBN 978-3-87907-622-2.

114. Laux, P.; Nguyen, P.N.B.; Cullmann, J.; Kunstmann, H. Impacts of Land-Use/Land-Cover Change and Climate Change on the Regional Climate in the Central Vietnam. In *Land Use and Climate Change Interactions in Central Vietnam: LUCCi*, 1st ed.; Nauditt, A., Ribbe, L., Eds.; Springer: Singapore, 2017; pp. 143–151. ISBN 978-981-10-2623-2.

115. Liu, Z.; Xiu, C.; Song, W. Landscape-Based Assessment of Urban Resilience and Its Evolution: A Case Study of the Central City of Shenyang. *Sustainability* **2019**, *11*, 2964. [CrossRef]